

Computation of invariant sets for discrete-time uncertain systems

Elias Khalife¹ | Dany Abou Jaoude²  | Mazen Farhood¹  | Pierre-Loic Garoche³

¹Kevin T. Crofton Department of Aerospace and Ocean Engineering, Virginia Tech, Blacksburg, Virginia, USA

²Department of Mechanical Engineering, American University of Beirut, Beirut, Lebanon

³ENAC, The French National University of Civil Aviation, Toulouse, France

Correspondence

Dany Abou Jaoude, Department of Mechanical Engineering, Maroun Semaan Faculty of Engineering and Architecture, American University of Beirut, Beirut, Lebanon.

Email: da107@aub.edu.lb

Funding information

Center for Unmanned Aircraft Systems under National Science Foundation (NSF), Grant/Award Number: CNS-1650465; ANR project FEANICES, Grant/Award Number: ANR-17-CE25-0018; Army Research Office (ARO), Grant/Award Number: W911NF-21-1-0250; Office of Naval Research (ONR), Grant/Award Number: N00014-18-1-2627; University Research Board (URB) at the American University of Beirut (AUB)

Abstract

This article proposes novel methods for the computation of state and output bounding sets for discrete-time uncertain systems. The systems under consideration are formed from the interconnection of a nominal linear time-invariant system and an uncertainty operator that is known to lie within a prespecified set. The set of allowable uncertainties is described by a pointwise integral quadratic constraint (IQC), that is, a quadratic constraint that holds for all time-steps. Examples of pointwise IQCs characterizing common uncertainty sets are provided. The exogenous input to the system is assumed to lie in a given polytope or ellipsoid for all time-steps. The proposed methods are illustrated via an example.

KEYWORDS

discrete-time uncertain systems, ellipsoidal invariants, integral quadratic constraints, S-procedure

1 | INTRODUCTION

This article deals with computing state and output bounding sets for discrete-time uncertain systems subject to persistent inputs bounded pointwise in time. The uncertain systems are modeled in a linear fractional transformation (LFT) framework, wherein the nominal part is a discrete-time linear time-invariant (LTI) system and the set of allowable uncertainty operators is characterized using the framework of integral quadratic constraints (IQCs). Specifically, the set of allowable uncertainties is assumed to satisfy a pointwise IQC, that is, a quadratic constraint that holds for all time-steps and relates the input and output of the operators in the uncertainty set. A classical IQC consists in the discrete-time setting of a constraint on an infinite summation of quadratic terms,¹ and so, a pointwise IQC is by definition more restrictive than its classical counterpart. Nonetheless, examples are provided of common uncertainty sets that admit pointwise IQC characterizations. The exogenous input affecting the uncertain system is assumed to lie in either one of two sets for all time-steps: (1) a convex, closed, and bounded polytope or (2) an ellipsoid. As with the works,^{2,3} the characterization of the exogenous input in terms of a constraint that holds for all time-steps is a distinctive feature of the proposed methods. In

comparison, other IQC-based approaches for the computation of invariant sets and operational envelopes for uncertain systems assume ℓ_2 -norm-bounded exogenous inputs,⁴⁻⁹ as is common practice in robust control.

The literature is rich in works that deal with the problem of computing invariant sets for control systems as well as related problems such as the computation of reachable sets and estimation of regions of attraction; see, for instance, the monograph¹⁰ and the references therein. Commonly used set representations include ellipsoids, polyhedral sets, and zonotopes. Ellipsoids are used to represent the bounding sets computed in the present work. Generally, ellipsoids allow for a simple set representation and the use of convex optimization tools. An important reference on the use of ellipsoids and linear matrix inequality (LMI) techniques for the computation of invariant sets is the seminal book.¹¹ Ellipsoidal modeling has also been used in reachability analysis;¹² see also the MATLAB toolbox,¹³ which implements the methods in Reference 14. Some recent relevant works that deal with discrete-time problem setups include the work¹⁵ in which the maximal contractive invariant ellipsoid is determined for multi-input systems with linear feedback subject to saturation, the work¹⁶ in which the attractive ellipsoid method is applied for the computation of robustly stabilizing state-feedback control laws for polytopic systems subject to control constraints and bounded perturbations, and the work¹⁷ which deals with the reachable set estimation problem (ellipsoidal over-approximation) for polytopic linear systems subject to peak-bounded disturbances and multiple constant delays. Polyhedral sets allow for a more complex representation of invariant sets; however, they are computed using complex iterative algorithms whose finite termination needs to be separately analyzed. One potential remedy is to look for low/fixed-complexity polytopic sets as was done in the works¹⁸⁻²⁰ for the computation of robust control invariant sets for discrete-time, constrained, uncertain systems subject to additive disturbances. The work¹⁸ deals with systems subject to norm-bounded uncertainty matrices, whereas the works^{19,20} deal with systems formulated in an LFT framework wherein the uncertainty matrix lies in a polytope. Zonotopes are a special class of polytopes, parameterized by a center and generators, which allow for some computationally cheaper operations involved in reachability analysis. Zonotopes are used in the MATLAB toolbox, CORA,²¹ for the over-approximation computation of reachable sets. Finally, in addition to the aforementioned convex set representations, it is possible to have nonconvex set representations; see for instance the survey paper²² and the recent paper²³ wherein sparse polynomial zonotopes are introduced as a new set representation for formal verification of hybrid systems.

Closely related to the present work are the works,⁴⁻⁹ which also employ the IQC framework, and the works^{17,21} on reachability analysis. While these works produce operating envelopes for uncertain systems, our work looks at the different analysis problem of computing state invariant and output bounding sets. The derived results make use of the S-procedure; see, for instance, the Reference 24. This allows for the extension of the results in the Reference 25, which deals with discrete-time LTI systems, to the class of uncertain systems in LFT form treated here and the integration of the IQC framework into the analysis. The adopted IQC framework allows for a systematic and unified treatment of multiple types of uncertainties, for example, static LTI, static linear time-varying (LTV), rate-bounded static LTV uncertainties, and uncertain time-varying time-delays, as well as sector-bounded nonlinearities, and combinations thereof, as long as they admit pointwise IQC characterizations. Our results allow for both static and dynamic IQC multipliers and filters in admissible IQC characterizations. As mentioned before, compared to the aforementioned IQC-based works, our results allow for persistent, bounded exogenous inputs, namely, inputs that lie in a given polytope or ellipsoid at all time-steps, as opposed to being restricted to finite energy inputs. In this regard, the works^{2,3} also employ the IQC framework and derive analysis results that allow for persistent bounded exogenous inputs. Motivated by problems in model predictive control, these works employ ρ -hard IQCs from Reference 26 and derive results for the computation of reachable sets for uncertain systems subject to inputs that are norm-bounded pointwise in time. Specifically, the works^{2,3} employ Finsler's lemma to extend the results in Reference 26, derived for the analysis of convergence of optimization algorithms, by accounting for exogenous inputs to the uncertain system. A preliminary version of this work appeared in the conference paper.²⁷ Therein, results are presented for computing state invariant sets for uncertain systems subject to inputs that lie in a polytope for all time-steps. The present work extends those results by allowing for computing both state and output bounding sets for uncertain systems subject to inputs that lie in a polytope or an ellipsoid for all time-steps. Additionally, the present work discusses the potential use of a multiconvexity relaxation technique for deriving alternative conditions to one condition in the results in Reference 27, which potentially can lead to a reduction in conservatism. This work also provides a list of uncertainty sets that admit pointwise IQC characterizations and explains how to modify the results to account for local pointwise IQCs describing the uncertainty sets. Moreover, this work discusses the computational complexity of the derived results through a practical example involving the analysis of a linear parameter-varying (LPV) controller designed for a small fixed-wing unmanned aircraft system. Finally, the paper provides a comprehensive illustrative example that showcases the applicability of the proposed results.

The work in this article is motivated by analysis problems that arise in hybrid control design and formal verification. For instance, an autonomous system may be modeled as a hybrid system consisting of a family of dynamic subsystems and a rule that drives the switching between these subsystems. A modular approach to solving the associated hybrid control problem entails designing subcontrollers locally for each constituent subsystem; see, for instance, the works.^{28,29} Then, the analysis results of this article can be used to guide the control design process to achieve some desired robust performance guarantees for the hybrid system by ensuring that the outputs of the controlled subsystems reside in matching invariant sets across switching boundaries. Also, these tools can potentially be used to formally verify the control software implementation. Specifically, they could be utilized to annotate the control code with statements in predicate logic based on the Floyd-Hoare paradigm, and then the annotated code can be checked for correctness by using a theorem prover; see, for instance, the seminal work.³⁰

The article is structured as follows. Section 2 gives the notation and S-procedure. Section 3 describes the considered classes of uncertain systems and exogenous inputs and gives the problem formulation. Sections 4 and 5 give the results pertaining to inputs bounded for all time-steps within polytopes and ellipsoids, respectively. Section 6 gives examples of uncertainty sets that can be characterized using pointwise IQCs. The illustrative example is given in Section 7, and the article concludes with Section 8.

2 | NOTATION AND PRELIMINARIES

The sets of nonnegative integers, reals, real-valued vectors of dimension n , and $n \times m$ real-valued matrices are denoted by \mathbb{N}_0 , \mathbb{R} , \mathbb{R}^n , and $\mathbb{R}^{n \times m}$, respectively. The $n \times m$ zero matrix and the $n \times n$ identity matrix are denoted by $0_{n \times m}$ and I_n , respectively. Given a vector $v \in \mathbb{R}^n$, $\text{diag}(v) = \text{diag}(v_1, \dots, v_n)$ denotes the diagonal matrix formed from the entries v_i of v . Let G be an LTI system. The quadruple (A, B, C, D) is used to denote a realization of G , which may also be represented as

$\left[\begin{array}{c|c} A & B \\ \hline C & D \end{array} \right]$. Let $A \in \mathbb{R}^{n \times m}$ and $B \in \mathbb{R}^{p \times q}$, and denote by a_{ij} the (i, j) th entry of A . The block-diagonal augmentation of A

and B is defined as $\text{blkdiag}(A, B) = \begin{bmatrix} A & 0_{n \times q} \\ 0_{p \times m} & B \end{bmatrix}$, and their Kronecker product is given by

$$A \otimes B = \begin{bmatrix} a_{11}B & \cdots & a_{1m}B \\ \vdots & \ddots & \vdots \\ a_{n1}B & \cdots & a_{nm}B \end{bmatrix} \in \mathbb{R}^{(n \times p) \times (m \times q)}.$$

The transpose of a matrix X is denoted by X^T . The sets of $n \times n$ symmetric matrices, positive semidefinite matrices, and positive definite matrices are denoted by \mathbb{S}^n , \mathbb{S}_+^n , and \mathbb{S}_{++}^n , respectively. Let $X \in \mathbb{S}^n$. We write $X \geq 0$, $X \leq 0$, $X > 0$, and $X < 0$ to mean that $X \in \mathbb{S}_+^n$, $-X \in \mathbb{S}_+^n$, $X \in \mathbb{S}_{++}^n$, and $-X \in \mathbb{S}_{++}^n$, respectively. With every $X \in \mathbb{S}_{++}^n$, we associate an ellipsoid $\mathcal{E}_X = \{x \in \mathbb{R}^n \mid x^T X x \leq 1\}$.

The symbol $\mathbb{RH}_\infty^{m \times n}$ denotes the space of $m \times n$ real, rational, matrix-valued functions, whose poles lie inside the open unit-disk in the complex plane. The symbol ℓ_{2e}^n denotes the space of real, vector-valued sequences $w = (w(0), w(1), \dots)$ such that $w(k) \in \mathbb{R}^n$ for all $k \in \mathbb{N}_0$. The Hilbert space ℓ_2^n is a subspace of ℓ_{2e}^n consisting of sequences w having a finite ℓ_2 -norm, defined by $\|w\|_{\ell_2^n}^2 = \sum_{k=0}^{\infty} \|w(k)\|_2^2$, where $\|w(k)\|_2 = \sqrt{w^T(k)w(k)}$ is the Euclidean norm. The symbols ℓ_{2e}^n and ℓ_2^n are often simplified to ℓ_{2e} and ℓ_2 , respectively.

Lemma 1 (S-procedure²⁴). Let $Q_i \in \mathbb{S}^m$, $s_i \in \mathbb{R}^m$, $r_i \in \mathbb{R}$ for $i = 0, 1, \dots, N$, and define the following quadratic functionals on \mathbb{R}^m : $\sigma_i(x) = x^T Q_i x + 2s_i^T x + r_i = \begin{bmatrix} x \\ 1 \end{bmatrix}^T \begin{bmatrix} Q_i & s_i \\ s_i^T & r_i \end{bmatrix} \begin{bmatrix} x \\ 1 \end{bmatrix}$. If there exist $\tau_i \geq 0$ for $i = 1, \dots, N$ such that $\sigma_0(x) - \sum_{i=1}^N \tau_i \sigma_i(x) \geq 0$ for all $x \in \mathbb{R}^m$, or equivalently,

$$\begin{bmatrix} Q_0 & s_0 \\ s_0^T & r_0 \end{bmatrix} - \sum_{i=1}^N \tau_i \begin{bmatrix} Q_i & s_i \\ s_i^T & r_i \end{bmatrix} \geq 0,$$

then it follows that $\sigma_0(x) \geq 0$ for all $x \in \mathbb{R}^m$ such that $\sigma_i(x) \geq 0$ for all $i = 1, \dots, N$.

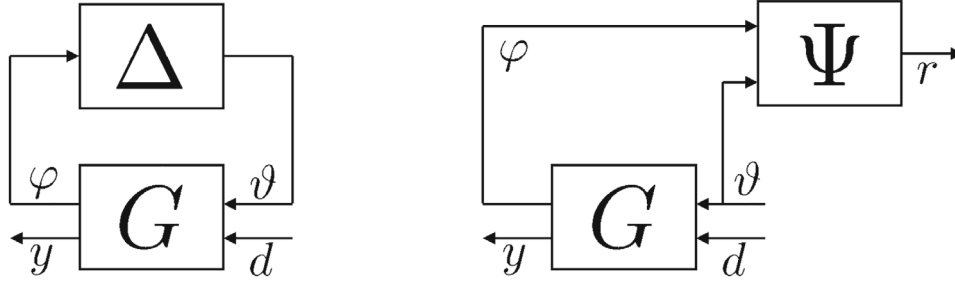


FIGURE 1 LFT system (G, Δ) (left) and augmented system H (right).

3 | PROBLEM FORMULATION

Consider the LFT system (G, Δ) in Figure 1, described by

$$\begin{aligned}
 x_G(k+1) &= A_G x_G(k) + B_{G1} \vartheta(k) + B_{G2} d(k), \\
 \varphi(k) &= C_{G1} x_G(k) + D_{G11} \vartheta(k) + D_{G12} d(k), \\
 y(k) &= C_{G2} x_G(k) + D_{G21} \vartheta(k) + D_{G22} d(k), \\
 \vartheta &= \Delta(\varphi),
 \end{aligned} \tag{1}$$

where $k \in \mathbb{N}_0$ denotes discrete time. The sequences x_G , d , and y denote the state, external input, and system output, respectively. As for the dimensions, $x_G(k) \in \mathbb{R}^{n_G}$, $d(k) \in \mathbb{R}^{n_d}$, $y(k) \in \mathbb{R}^{n_y}$, $\varphi(k) \in \mathbb{R}^{n_\varphi}$, and $\vartheta(k) \in \mathbb{R}^{n_\vartheta}$. The nominal system $G = \begin{bmatrix} G_{11} & G_{12} \\ G_{21} & G_{22} \end{bmatrix} : \ell_{2e}^{n_\vartheta} \times \ell_{2e}^{n_d} \rightarrow \ell_{2e}^{n_\varphi} \times \ell_{2e}^{n_y}$ is assumed to be a stable discrete-time LTI system. The uncertainty operator $\Delta : \ell_{2e}^{n_\varphi} \rightarrow \ell_{2e}^{n_\vartheta}$ is assumed to be causal and bounded and lies within a prespecified set $\mathbf{\Delta}$. The uncertain system $(G, \mathbf{\Delta})$ is assumed to be well-posed. $(G, \mathbf{\Delta})$ is well-posed if, for all $\Delta \in \mathbf{\Delta}$ and $d \in \ell_{2e}^{n_d}$, there exist unique solutions $x_G \in \ell_{2e}^{n_G}$, $\varphi \in \ell_{2e}^{n_\varphi}$, $\vartheta \in \ell_{2e}^{n_\vartheta}$, and $y \in \ell_{2e}^{n_y}$ to (1) that causally depend on d .

In this article, we treat the problem of finding ellipsoidal sets in which $x_G(k)$ and $y(k)$ lie for all $k \in \mathbb{N}_0$, given that $x_G(0)$ and $d(k)$ for all $k \in \mathbb{N}_0$ lie in prespecified sets. The uncertainty set $\mathbf{\Delta}$ is assumed to satisfy a pointwise IQC, as defined next.

Definition 1. Let $\Psi \in \mathbb{RH}_\infty^{n_r \times (n_\varphi + n_\vartheta)}$ and $S \in \mathbb{S}^{n_r}$ for some positive integer n_r . The set $\mathbf{\Delta}$ is said to satisfy the pointwise IQC defined by (Ψ, S) , or $\mathbf{\Delta} \in \text{pwIQC}(\Psi, S)$ for short, if the quadratic inequality

$$r^T(k) S r(k) \geq 0, \tag{2}$$

holds for all $k \in \mathbb{N}_0$, $\varphi \in \ell_{2e}^{n_\varphi}$, $\vartheta = \Delta(\varphi) \in \ell_{2e}^{n_\vartheta}$, and $\Delta \in \mathbf{\Delta}$, where

$$\begin{aligned}
 x_\Psi(k+1) &= A_\Psi x_\Psi(k) + B_{\Psi1} \varphi(k) + B_{\Psi2} \vartheta(k), \\
 r(k) &= C_\Psi x_\Psi(k) + D_{\Psi1} \varphi(k) + D_{\Psi2} \vartheta(k), \\
 x_\Psi(0) &= 0, \quad x_\Psi(k) \in \mathbb{R}^{n_\Psi}, \quad r(k) \in \mathbb{R}^{n_r}.
 \end{aligned} \tag{3}$$

Examples of uncertainty sets $\mathbf{\Delta}$ that admit pointwise IQC characterizations are given in Section 6.

To derive the results in this article, an LTI augmented system H is constructed, as illustrated in Figure 1. For all $k \in \mathbb{N}_0$, the state-space equations of system H are given by

$$\begin{aligned}
 x_H(k+1) &= A_H x_H(k) + B_{H1} \vartheta(k) + B_{H2} d(k), \\
 r(k) &= C_{H1} x_H(k) + D_{H11} \vartheta(k) + D_{H12} d(k), \\
 y(k) &= C_{H2} x_H(k) + D_{H21} \vartheta(k) + D_{H22} d(k),
 \end{aligned} \tag{4}$$

with $x_H(k) = (x_G(k), x_\Psi(k))$,

$$\begin{aligned} A_H &= \begin{bmatrix} A_G & 0 \\ B_{\Psi_1} C_{G1} & A_\Psi \end{bmatrix}, & B_{H1} &= \begin{bmatrix} B_{G1} \\ B_{\Psi_1} D_{G11} + B_{\Psi_2} \end{bmatrix}, & B_{H2} &= \begin{bmatrix} B_{G2} \\ B_{\Psi_1} D_{G12} \end{bmatrix}, \\ C_{H1} &= \begin{bmatrix} D_{\Psi_1} C_{G1} & C_\Psi \end{bmatrix}, & D_{H11} &= D_{\Psi_1} D_{G11} + D_{\Psi_2}, & D_{H12} &= D_{\Psi_1} D_{G12}, \\ C_{H2} &= \begin{bmatrix} C_{G2} & 0 \end{bmatrix}, & D_{H21} &= D_{G21}, & D_{H22} &= D_{G22}. \end{aligned}$$

Two sets of input signals d are considered. Given a convex, closed, and bounded polytope $\Gamma \subseteq \mathbb{R}^{n_d}$, the first set is defined as

$$\mathbf{D}_\Gamma = \{d \in \mathcal{E}_{2e}^{n_d} \mid d(k) \in \Gamma \text{ for all } k \in \mathbb{N}_0\}. \quad (5)$$

Let $V = \{v_1, \dots, v_p\}$, for some integer $p \geq 1$, denote the set of vertices of Γ . Then, Γ is the convex hull of V .

Given an ellipsoid $\mathcal{E}_\Lambda = \{z \in \mathbb{R}^{n_d} \mid z^T \Lambda z \leq 1\}$, where $\Lambda \in \mathbb{S}_{++}^{n_d}$, the second set of allowable input signals d considered in this work is denoted by \mathbf{D}_Λ and defined as

$$\mathbf{D}_\Lambda = \{d \in \mathcal{E}_{2e}^{n_d} \mid d(k) \in \mathcal{E}_\Lambda \text{ for all } k \in \mathbb{N}_0\}. \quad (6)$$

The problem addressed in this article is to find $W \in \mathbb{S}_{++}^{n_G}$ and $Q \in \mathbb{S}_{++}^{n_y}$ such that if $x_G(0) \in \mathcal{E}_W$, then $x_G(k) \in \mathcal{E}_W$ and $y(k) \in \mathcal{E}_Q$ for all $k \in \mathbb{N}_0$, $\Delta \in \mathbf{\Delta}$, and d in the set \mathbf{D}_Γ or \mathbf{D}_Λ . To address this problem, the equations of system H are considered, and matrices $P \in \mathbb{S}_{++}^{n_G+n_\Psi}$, $W \in \mathbb{S}_{++}^{n_G}$, and $Q \in \mathbb{S}_{++}^{n_y}$ are found such that if $x_H(0) \in \mathcal{E}_P$, then $x_H(k) \in \mathcal{E}_P$, $x_G(k) \in \mathcal{E}_W$, and $y(k) \in \mathcal{E}_Q$ for all $k \in \mathbb{N}_0$, d in \mathbf{D}_Γ or \mathbf{D}_Λ , and $\vartheta \in \mathcal{E}_{2e}^{n_\vartheta}$ such that the output r of system H satisfies $r^T(k) S r(k) \geq 0$ for all $k \in \mathbb{N}_0$. Since $\mathbf{\Delta} \in \text{pwIQC}(\Psi, S)$, a special case of such signals ϑ are those generated from the uncertain system equations, that is, $\vartheta = \Delta(\varphi)$, $\Delta \in \mathbf{\Delta}$, and

$$\varphi(k) = C_{G1} x_G(k) + D_{G11} \vartheta(k) + D_{G12} d(k) = [C_{G1} \quad 0] x_H(k) + D_{G11} \vartheta(k) + D_{G12} d(k), \quad (7)$$

for all $k \in \mathbb{N}_0$. Thus, this indirect approach gives us bounding sets for the augmented system H that are also valid for the uncertain system $(G, \mathbf{\Delta})$. Let P_{11} denote the $(1, 1)$ -block of P when partitioned conformably with the partitioning of $x_H(k)$. The zero initial condition, $x_\Psi(0) = 0$, of the IQC filter Ψ is used to express the condition $x_H(0) \in \mathcal{E}_P$ equivalently as $x_G(0) \in \mathcal{E}_{P_{11}}$. Thus, the computed positive definite matrices P , W , and Q are such that $x_G(0) \in \mathcal{E}_{P_{11}}$ implies that $x_H(k) \in \mathcal{E}_P$, $x_G(k) \in \mathcal{E}_W$, and $y(k) \in \mathcal{E}_Q$ for all $k \in \mathbb{N}_0$, $\Delta \in \mathbf{\Delta}$, and d in \mathbf{D}_Γ or \mathbf{D}_Λ .

4 | STATE AND OUTPUT BOUNDING SETS: POINTWISE POLYTOPIC INPUT CONSTRAINTS

This section treats the problem of finding bounding sets for the uncertain system $(G, \mathbf{\Delta})$, where $\mathbf{\Delta} \in \text{pwIQC}(\Psi, S)$ and $d \in \mathbf{D}_\Gamma$. Theorem 1 summarizes the results in Reference 27 for computing state bounding sets. Theorem 2 provides extensions for computing output bounding sets.

Theorem 1 (27). *Consider the uncertain system $(G, \mathbf{\Delta})$ defined in (1) with state x_G such that $\mathbf{\Delta} \in \text{pwIQC}(\Psi, S)$ and the corresponding augmented system H defined in (4) with state x_H .*

(a) *If there exist $P \in \mathbb{S}_{++}^{n_G+n_\Psi}$, $\tau_1 \geq 0$, and $\tau_2 \geq 0$ such that*

$$\begin{aligned} & \begin{bmatrix} - \begin{bmatrix} A_H^T \\ B_{H1}^T \end{bmatrix} P \begin{bmatrix} A_H & B_{H1} \end{bmatrix} & - \begin{bmatrix} A_H^T \\ B_{H1}^T \end{bmatrix} P B_{H2} v_i \\ - v_i^T B_{H2}^T P \begin{bmatrix} A_H & B_{H1} \end{bmatrix} & 1 - v_i^T B_{H2}^T P B_{H2} v_i \end{bmatrix} - \tau_1 \text{blkdiag} \left(- \begin{bmatrix} I \\ 0 \end{bmatrix} P \begin{bmatrix} I & 0 \end{bmatrix}, 1 \right) \\ & - \tau_2 \begin{bmatrix} \begin{bmatrix} C_{H1}^T \\ D_{H11}^T \end{bmatrix} S \begin{bmatrix} C_{H1} & D_{H11} \end{bmatrix} & \begin{bmatrix} C_{H1}^T \\ D_{H11}^T \end{bmatrix} S D_{H12} v_i \\ v_i^T D_{H12}^T S \begin{bmatrix} C_{H1} & D_{H11} \end{bmatrix} & v_i^T D_{H12}^T S D_{H12} v_i \end{bmatrix} \succeq 0, \end{aligned} \tag{8}$$

for all the vertices of Γ , that is, $v_i \in V$, and

$$B_{H2}^T P B_{H2} + \tau_2 D_{H12}^T S D_{H12} \succeq 0, \tag{9}$$

then $x_H^T(0) P x_H(0) \leq 1$ implies that $x_H^T(k) P x_H(k) \leq 1$ for all $k \in \mathbb{N}_0$, $\Delta \in \mathbf{\Delta}$, and $d \in \mathbf{D}_\Gamma$, where \mathbf{D}_Γ is defined in (5).

(b) If there exist $P \in \mathbb{S}_{++}^{n_G+n_\Psi}$, $W \in \mathbb{S}_{++}^{n_G}$, $\tau_1 \geq 0$, $\tau_2 \geq 0$, and $\tau_3 \geq 0$ that satisfy (8) for all $v_i \in V$, (9), and

$$\begin{bmatrix} -E^T W E & 0 \\ 0 & 1 \end{bmatrix} - \tau_3 \begin{bmatrix} -P & 0 \\ 0 & 1 \end{bmatrix} \succeq 0, \tag{10}$$

where $E = \begin{bmatrix} I_{n_G} & 0_{n_G \times n_\Psi} \end{bmatrix}$, then $x_H^T(0) P x_H(0) \leq 1$ implies that $x_G^T(k) W x_G(k) \leq 1$ for all $k \in \mathbb{N}_0$, $\Delta \in \mathbf{\Delta}$, and $d \in \mathbf{D}_\Gamma$.

Imposing (9) in addition to (8) at the vertices of Γ ensures that (8) holds for all $\hat{d} \in \Gamma$. Remark 2 shows how to use the multiconvexity relaxation technique to obtain other, potentially less conservative conditions than (9). If Γ is symmetric, that is, $-\Gamma = \{-\hat{d} \mid \hat{d} \in \Gamma\} = \Gamma$, (8) needs to be imposed only at half of the vertices since (8) holds at vertex v_i if and only if it holds at vertex $v_j = -v_i$.

The IQC filter Ψ is typically fixed a priori and the IQC variables in S often appear linearly. Thus, when solving the inequalities in Theorem 1, one solves for $\hat{S}_2 = \tau_2 S$ by lumping $\tau_2 \geq 0$ with the variables in S , which eliminates the nonlinearity due to the multiplication between τ_2 and S . The remaining source of non-convexity in (8) is the multiplication between τ_1 and P , which can be handled by gridding over τ_1 . For a fixed τ_1 , (8) is an LMI in P and the variables in \hat{S}_2 . Moreover, $\tau_1 \in [0, 1]$ since (9) is imposed. If Ψ is a static operator, solving (8) and (9) yields a state invariant set for the uncertain system $(G, \mathbf{\Delta})$. In this case, $x_H = x_G$ and $P \in \mathbb{S}_{++}^{n_G}$, and so, if $x_G(0) \in \mathcal{E}_P$, then $x_G(k) \in \mathcal{E}_P$ for all $k \in \mathbb{N}_0$, $\Delta \in \mathbf{\Delta}$, and $d \in \mathbf{D}_\Gamma$. If Ψ is a dynamic operator, solving (8) and (9) yields a state invariant set for the augmented system H : if $x_H(0) \in \mathcal{E}_P$, then $x_H(k) \in \mathcal{E}_P$ for all $k \in \mathbb{N}_0$, φ defined as per (7), $\vartheta = \Delta(\varphi)$, $\Delta \in \mathbf{\Delta}$, and $d \in \mathbf{D}_\Gamma$. In this case, (10) can be further imposed to conclude that $x_G(k) \in \mathcal{E}_W$ for all $k \in \mathbb{N}_0$, $\Delta \in \mathbf{\Delta}$, and $d \in \mathbf{D}_\Gamma$. Since $x_\Psi(0) = 0$, then $x_H(0) \in \mathcal{E}_P$ if and only if $x_G(0) \in \mathcal{E}_{P_{11}}$, where $P = [P_{ij}]_{i,j=1,2}$ is partitioned conformably with the partitioning of $x_H(k) = (x_G(k), x_\Psi(k))$. Thus, by solving (8)–(10), we conclude that if $x_G(0) \in \mathcal{E}_{P_{11}}$, then $x_G(k) \in \mathcal{E}_W$ for all $k \in \mathbb{N}_0$, $\Delta \in \mathbf{\Delta}$, and $d \in \mathbf{D}_\Gamma$. In this article, we take $W = P_{11} - P_{12} P_{22}^{-1} P_{12}^T > 0$ (this choice of P and W satisfies (10) for $\tau_3 = 1$). In this case, the ellipsoid $\mathcal{E}_W = \{\hat{x} \in \mathbb{R}^{n_G} \mid \hat{x} = E x, x \in \mathcal{E}_P\}$ is a projection of \mathcal{E}_P .

Remark 1. The conditions in Theorem 1 clearly imply the robust uniform stability of the the uncertain system $(G, \mathbf{\Delta})$. Namely, $(G, \mathbf{\Delta})$ is robustly uniformly stable if it is well-posed and there exists a constant scalar $c \geq 0$ such that $\|x_G(k)\|_2 \leq c \|x_G(0)\|_2$ for any $x_G(0) \in \mathbb{R}^{n_G}$, $k \in \mathbb{N}_0$, $\Delta \in \mathbf{\Delta}$, and $d \equiv 0$. This is not difficult to see since if there exist $P \in \mathbb{S}_{++}^{n_G+n_\Psi}$, $\tau_1 \geq 0$, and $\tau_2 \geq 0$ such that (8) holds for all the vertices of Γ , then the inequality

$$\begin{bmatrix} A_H^T P A_H - P & A_H^T P B_{H1} \\ B_{H1}^T P A_H & B_{H1}^T P B_{H1} \end{bmatrix} + \tau_2 \begin{bmatrix} C_{H1}^T \\ D_{H11}^T \end{bmatrix} S \begin{bmatrix} C_{H1} & D_{H11} \end{bmatrix} \preceq 0 \tag{11}$$

holds, which implies the robust uniform stability of the system³¹ with $c = \sqrt{\text{cond}(P)}$, where $\text{cond}(P)$ is the condition number of P . Furthermore, if the solutions P and $\tau_2 S$ are such that (11) holds with

strict inequality, then the system is robustly asymptotically stable,^{5(Theorem 1)} that is, the solutions to (1) are in ℓ_2 for $d \in \ell_2^{n_d}$, and the system equations define a bounded causal mapping from d to (x_G, y) for all $\Delta \in \Delta$.

Remark 2. It is possible to use the multiconvexity relaxation technique³² to derive other sufficient conditions, potentially less conservative than (9), that ensure that (8) holds for all $\hat{d} \in \Gamma$ if it holds for all $v_i \in V$. For example, assume that Γ is a hyper-rectangle, that is, $\Gamma = \{\hat{d} \in \mathbb{R}^{n_d} \mid l_j \leq \hat{d}_j \leq u_j \text{ for } j = 1, \dots, n_d\}$, where \hat{d}_j is the j th component of \hat{d} . Let $Z = (P, \hat{S}_2)$, where $\hat{S}_2 = \tau_2 S$, and define the matrix-valued function $\mathcal{L}_{\tau_1}(\cdot, \cdot)$ such that (8) can be expressed as $\mathcal{L}_{\tau_1}(Z, v_i) \leq 0$. By Theorem 1, to find a state bounding ellipsoid for (G, Δ) , it is required to find appropriate τ_1 and Z such that $\mathcal{L}_{\tau_1}(Z, \hat{d}) \leq 0$ for all $\hat{d} \in \Gamma$. For a fixed τ_1 , $\mathcal{L}_{\tau_1}(Z, \hat{d}) \leq 0$ is a parameterized LMI in Z , where \hat{d} is the parameter. It is possible to write

$$\mathcal{L}_{\tau_1}(Z, \hat{d}) = M_{0, \tau_1}(Z) + \sum_{j=1}^{n_d} \hat{d}_j M_{j, \tau_1}(Z) + \sum_{j,m=1}^{n_d} \hat{d}_j \hat{d}_m M_{j,m, \tau_1}(Z),$$

where $M_{0, \tau_1}(\cdot)$, $M_{j, \tau_1}(\cdot)$, and $M_{j,m, \tau_1}(\cdot)$ are appropriately defined real, symmetric, matrix-valued and linear functions of Z . By the results in Reference 32 (Section 4.1) dealing with parameterized LMIs with quadratic parameter dependence, for a given τ_1 , it follows that $\mathcal{L}_{\tau_1}(Z, \hat{d}) \leq 0$ for all $\hat{d} \in \Gamma$ if $\mathcal{L}_{\tau_1}(Z, v_i) \leq 0$ for all $v_i \in V$ and $M_{j,j, \tau_1}(Z) \geq 0$ for $j = 1, \dots, n_d$. By introducing additional variables $\lambda_j \geq 0$ for all $j = 1, \dots, n_d$ and imposing the constraint $\mathcal{L}_{\tau_1}(Z, v_i) \leq -\sum_{j=1}^{n_d} (v_i)_j^2 \lambda_j I$ for all $v_i \in V$, the multiconvexity constraints can be relaxed to $M_{j,j, \tau_1}(Z) \geq -\lambda_j I$ for $j = 1, \dots, n_d$.

Remark 3. It is possible to incorporate local pointwise IQCs³³ into the conditions of Theorem 1. The advantage of using local IQCs is that they provide a more accurate characterization of the uncertainties in the operating region of interest. For instance, in the case of sector-bounded nonlinearities, it is possible to derive tighter sector bounds on local intervals. Suppose Δ satisfies the local pointwise IQC defined by $(\Psi_{\text{loc}}, S_{\text{loc}})$ when the j th element of $\varphi(k)$, denoted by $\varphi_j(k)$, is restricted to the interval $[-\bar{\varphi}_j, \bar{\varphi}_j]$ with $\bar{\varphi}_j \geq 0$ for $j = 1, \dots, n_\varphi$. Then, the S-procedure can be used to ensure that the elements of $\varphi(k)$ are indeed restricted to their local intervals. To this end, for $j = 1, \dots, n_\varphi$, we define three quadratic functions $\bar{\sigma}_{0, \hat{d}}(x)$, $\bar{\sigma}_1(x)$, and $\bar{\sigma}_{2, \hat{d}}(x)$ such that, for $\xi(k) = (x_H(k), \vartheta(k))$, the inequalities $\bar{\sigma}_{0, \hat{d}}(\xi(k)) \geq 0$, $\bar{\sigma}_1(\xi(k)) \geq 0$, and $\bar{\sigma}_{2, \hat{d}}(\xi(k)) \geq 0$ are equivalent to $(\varphi_j(k))^2 \leq \bar{\varphi}_j^2$, that is, $|\varphi_j(k)| \leq \bar{\varphi}_j$, $x_H^T(k) P x_H(k) \leq 1$, and $r^T(k) S_{\text{loc}, j} r(k) \geq 0$, respectively, where $S_{\text{loc}, j}$ is a copy of S_{loc} associated with φ_j . Then, using Lemma 1, we derive a matrix inequality similar to (8), parameterized by the vertices $v_i \in V$ of the polytope Γ . To ensure that this inequality holds for all $d(k) \in \Gamma$ rather than just at $v_i \in V$, we impose an inequality similar to (9). Hence, given the bounds on the components $\varphi_j(k)$ of $\varphi(k)$, these inequalities can be enforced alongside the inequalities of Theorem 1, where S is substituted with S_{loc} . If $D_{G11} = 0$, the quadratic function $\bar{\sigma}_{2, \hat{d}}(x)$ is dropped and the resulting inequalities simplify. In this case, an alternative approach inspired by the work in Reference 33 can also be implemented. Namely, in addition to the conditions in Theorem 1, we enforce the following inequalities: $\bar{\varphi}_j \geq \bar{d}_j$ and

$$\begin{bmatrix} (\bar{\varphi}_j - \bar{d}_j)^2 & [C_{G1}^{(j)} \quad 0] \\ [C_{G1}^{(j)} \quad 0]^T & P \end{bmatrix} \geq 0, \quad (12)$$

for $j = 1, \dots, n_\varphi$, where $\bar{d}_j = \max_{d(k) \in \Gamma} (|D_{G12}^{(j)} d(k)|)$ and $C_{G1}^{(j)}$ and $D_{G12}^{(j)}$ denote the j th rows of C_{G1} and D_{G12} , respectively. These conditions are derived by applying^{34(Lemma 1)} to Equation (7), while taking into account that $D_{G11} = 0$ and $d(k) \in \Gamma$ for all $k \in \mathbb{N}_0$.

Theorem 2. Consider the uncertain system (G, Δ) defined in (1) with state x_G and output y such that $\Delta \in \text{pwIQC}(\Psi, S)$ and the corresponding augmented system H defined in (4) with state x_H . Let $P \in \mathbb{S}_{++}^{n_G + n_\Psi}$. If there

exist $Q \in \mathbb{S}_{++}^{n_y}$, $\tau_4 \geq 0$, and $\tau_5 \geq 0$ such that

$$\begin{aligned} & \begin{bmatrix} - \begin{bmatrix} C_{H2}^T \\ D_{H21}^T \end{bmatrix} Q \begin{bmatrix} C_{H2} & D_{H21} \end{bmatrix} & - \begin{bmatrix} C_{H2}^T \\ D_{H21}^T \end{bmatrix} Q D_{H22} v_i \\ - v_i^T D_{H22}^T Q \begin{bmatrix} C_{H2} & D_{H21} \end{bmatrix} & 1 - v_i^T D_{H22}^T Q D_{H22} v_i \end{bmatrix} - \tau_4 \text{blkdiag} \left(- \begin{bmatrix} I \\ 0 \end{bmatrix} P \begin{bmatrix} I & 0 \end{bmatrix}, 1 \right) \\ & - \tau_5 \begin{bmatrix} \begin{bmatrix} C_{H1}^T \\ D_{H11}^T \end{bmatrix} S \begin{bmatrix} C_{H1} & D_{H11} \end{bmatrix} & \begin{bmatrix} C_{H1}^T \\ D_{H11}^T \end{bmatrix} S D_{H12} v_i \\ v_i^T D_{H12}^T S \begin{bmatrix} C_{H1} & D_{H11} \end{bmatrix} & v_i^T D_{H12}^T S D_{H12} v_i \end{bmatrix} \succcurlyeq 0, \end{aligned} \tag{13}$$

for all the vertices v_i of Γ and

$$D_{H22}^T Q D_{H22} + \tau_5 D_{H12}^T S D_{H12} \succcurlyeq 0, \tag{14}$$

then, for any $k \in \mathbb{N}_0$, $x_H^T(k) P x_H(k) \leq 1$ implies that $y^T(k) Q y(k) \leq 1$ for all $\Delta \in \mathbf{\Delta}$ and $d(k) \in \Gamma$.

Proof. We begin by defining the quadratic functions

$$\begin{aligned} \hat{\sigma}_1(x) &= \begin{bmatrix} x \\ 1 \end{bmatrix}^T \text{blkdiag} \left(- \begin{bmatrix} I \\ 0 \end{bmatrix} P \begin{bmatrix} I & 0 \end{bmatrix}, 1 \right) \begin{bmatrix} x \\ 1 \end{bmatrix}, \\ \hat{\sigma}_{0,\hat{d}}(x) &= \begin{bmatrix} x \\ 1 \end{bmatrix}^T \begin{bmatrix} - \begin{bmatrix} C_{H2}^T \\ D_{H21}^T \end{bmatrix} Q \begin{bmatrix} C_{H2} & D_{H21} \end{bmatrix} & - \begin{bmatrix} C_{H2}^T \\ D_{H21}^T \end{bmatrix} Q D_{H22} \hat{d} \\ - \hat{d}^T D_{H22}^T Q \begin{bmatrix} C_{H2} & D_{H21} \end{bmatrix} & 1 - \hat{d}^T D_{H22}^T Q D_{H22} \hat{d} \end{bmatrix} \begin{bmatrix} x \\ 1 \end{bmatrix}, \\ \hat{\sigma}_{2,\hat{d}}(x) &= \begin{bmatrix} x \\ 1 \end{bmatrix}^T \begin{bmatrix} \begin{bmatrix} C_{H1}^T \\ D_{H11}^T \end{bmatrix} S \begin{bmatrix} C_{H1} & D_{H11} \end{bmatrix} & \begin{bmatrix} C_{H1}^T \\ D_{H11}^T \end{bmatrix} S D_{H12} \hat{d} \\ \hat{d}^T D_{H12}^T S \begin{bmatrix} C_{H1} & D_{H11} \end{bmatrix} & \hat{d}^T D_{H12}^T S D_{H12} \hat{d} \end{bmatrix} \begin{bmatrix} x \\ 1 \end{bmatrix}. \end{aligned}$$

Define $\xi(k) = (x_H(k), \vartheta(k))$. Then, it is not difficult to see that $\hat{\sigma}_{0,d(k)}(\xi(k)) \geq 0$, $\hat{\sigma}_1(\xi(k)) \geq 0$, and $\hat{\sigma}_{2,d(k)}(\xi(k)) \geq 0$ if and only if $y^T(k) Q y(k) \leq 1$, $x_H^T(k) P x_H(k) \leq 1$, and $r^T(k) S r(k) \geq 0$, respectively.

$x_H^T(k) P x_H(k) \leq 1$ holds by assumption, and $r^T(k) S r(k) \geq 0$ holds for all $k \in \mathbb{N}_0$ and $d(k)$ since $\mathbf{\Delta} \in \text{pwlQC}(\Psi, S)$. Since (14) is imposed, it follows that (13) holds for all $d(k) \in \Gamma$ and not only at $v_i \in V$. To see this, (13) is expressed as

$$\tilde{M}(v_i) = \begin{bmatrix} \tilde{M}_{11} & \tilde{M}_{12} v_i \\ v_i^T \tilde{M}_{12}^T & \tilde{m}_{22} - v_i^T \tilde{M}_{22} v_i \end{bmatrix} \succcurlyeq 0,$$

where $\tilde{m}_{22} = 1 - \tau_4$ and $\tilde{M}_{22} = D_{H22}^T Q D_{H22} + \tau_5 D_{H12}^T S D_{H12}$. It is desired to show that $\tilde{M}(v_i) \succcurlyeq 0$ for all $v_i \in V$ and $\tilde{M}_{22} \succcurlyeq 0$ (by (14)) imply that $\tilde{M}(d(k)) \succcurlyeq 0$ for all $d(k) \in \Gamma$. For any $d(k) \in \Gamma$, there exist $c_i \geq 0$ for $i = 1, \dots, p$ such that $\sum_i c_i = 1$ and $d(k) = \sum_i c_i v_i$. Then, $\tilde{M}(d(k)) = \sum_{i=1}^p c_i \tilde{M}(v_i) + \text{blkdiag}(0, \tilde{x})$, where $\tilde{x} = -d^T(k) \tilde{M}_{22} d(k) + \sum_i c_i v_i^T \tilde{M}_{22} v_i$. Thus, $\tilde{M}(d(k)) \succcurlyeq 0$ since $\tilde{x} \geq 0$ and $c_i \geq 0$ and $\tilde{M}(v_i) \succcurlyeq 0$ for all $i = 1, \dots, p$. That $\tilde{x} \geq 0$ follows from the convexity of the function $f(x) = x^T \tilde{M}_{22} x$ and Jensen's inequality,¹¹ that is, $f(d(k)) = f(\sum_i c_i v_i) \leq \sum_i c_i f(v_i)$.

Since (13) holds for all $d(k) \in \Gamma$, it follows from the S-procedure that $\hat{\sigma}_{0,d(k)}(\xi(k)) \geq 0$ whenever $\hat{\sigma}_1(\xi(k)) \geq 0$ and $\hat{\sigma}_{2,d(k)}(\xi(k)) \geq 0$ for all $d(k) \in \Gamma$ as desired. ■

Theorem 2 states that, for a given $P > 0$, if there exist $Q > 0$, $\tau_4 \geq 0$, and $\tau_5 \geq 0$ that satisfy (14) and (13) for all $v_i \in V$, then, for any $k \in \mathbb{N}_0$, $x_H(k) \in \mathcal{E}_P$ implies that $y(k) \in \mathcal{E}_Q$ for all $d(k) \in \Gamma$ and $\Delta \in \mathbf{\Delta}$. Note that it may be possible to obtain less conservative constraints than (14) by using the multiconvexity relaxation technique explained in Remark 2.

If P is obtained from Theorem 1, the conclusion from Theorem 2 is strengthened to: $x_H(0) \in \mathcal{E}_P$ implies that $y(k) \in \mathcal{E}_Q$ for all $k \in \mathbb{N}_0$, $\Delta \in \mathbf{\Delta}$, and $d \in \mathbf{D}_\Gamma$. Thus, Theorems 1 and 2 can be applied to compute positive definite matrices P and Q such that if $x_G(0) \in \mathcal{E}_{P_{11}}$, then $x_G(k) \in \mathcal{E}_W$, $x_H(k) \in \mathcal{E}_P$, and $y(k) \in \mathcal{E}_Q$ for all $k \in \mathbb{N}_0$, $\Delta \in \mathbf{\Delta}$, and $d \in \mathbf{D}_\Gamma$, where $W = P_{11} - P_{12}P_{22}^{-1}P_{12}^T$.

There are two possible ways for computing P and Q . One may first find $P > 0$, $\tau_1 \geq 0$, and $\tau_2 \geq 0$ that satisfy (8) for all $v_i \in V$ and (9), and then use the found P to solve for $Q > 0$, $\tau_4 \geq 0$, and $\tau_5 \geq 0$ that satisfy (13) for all $v_i \in V$ and (14). Alternatively, one may simultaneously solve for $P > 0$, $Q > 0$, and nonnegative τ_1 , τ_2 , τ_4 , and τ_5 that satisfy (8) and (13) for all $v_i \in V$, (9), and (14). In both cases, the problems at hand are formulated as semidefinite programs (SDPs) and solved using convex optimization tools. If P and Q are found sequentially, the problem in the first step, which yields a state bounding ellipsoid, is rendered convex by gridding over τ_1 , and the problem in the second step, which yields the corresponding output bounding ellipsoid, is convex. If P and Q are solved for simultaneously, double gridding over both τ_1 and τ_4 is required. Coarse grids are first used to estimate the location of the optimal point, followed by finer grids to obtain accurate results. In this work, the minimum volume output bounding ellipsoid \mathcal{E}_Q is sought by minimizing $-\log(\det(Q))$. When P and Q are found separately, the volume of the state bounding ellipsoid \mathcal{E}_W is minimized in the first step, where $W = P_{11} - P_{12}P_{22}^{-1}P_{12}^T$. To minimize the volume of \mathcal{E}_W , an auxiliary matrix $0 < \overline{W} \preceq W$ is introduced and the negative of its log-determinant is minimized. The constraint $\overline{W} \preceq W$ is equivalently re-written as the following LMI:

$$\begin{bmatrix} \overline{W} - P_{11} & P_{12} \\ P_{12}^T & -P_{22} \end{bmatrix} \preceq 0.$$

Simultaneously solving for P and Q yields a lower objective function value $-\log(\det(Q))$ than first optimizing P by minimizing $-\log(\det(\overline{W}))$ and then optimizing Q for the found P . This improvement comes at the expense of having to double-grid over τ_1 and τ_4 . In the example of Section 7, a minimal improvement in the objective function value is observed when simultaneously optimizing P and Q , which does not justify the incurred increase in the computational cost. Therefore, we only focus on the sequential solution approach in this article.

Remark 4. The optimization problems formulated from Theorems 1 and 2 can be generally expressed as vector optimization problems over the positive semidefinite cone. Specifically, the vector optimization problem obtained by applying Theorem 1 is

$$\begin{aligned} & \text{minimize (w.r.t. } \mathbb{S}_+^n) && f_0(P) \\ & \text{subject to} && P > 0, \tau_1 \geq 0, \tau_2 \geq 0, \\ & && (9), \text{ and } (8) \text{ imposed for all } v_i \in V, \end{aligned}$$

where $f_0 : \mathbb{S}^n \mapsto \mathbb{S}^n$ is defined by $f_0(P) = P^{-1}$ with domain $\text{dom}(f_0) = \mathbb{S}_{++}^n$. As discussed in the book,¹¹ Pareto optimal points can be obtained for this problem using scalarization. Different scalarizations can be used; for instance, in this article, the scalarized problems considered consist of minimizing $\log \det(f_0(P))$, $\log \det(f_0(\overline{W}))$, or $\log \det(f_0(Q))$, which can be interpreted as minimizing the volume of the corresponding ellipsoid, and we have found that to yield satisfactory results for our considered examples. It is also possible to minimize $\text{trace}(f_0(P))$ and to impose shape constraints on the ellipsoids based on the specific problem of interest.

5 | STATE AND OUTPUT BOUNDING SETS: POINTWISE ELLIPSOIDAL INPUT CONSTRAINTS

This section treats the problem of finding bounding sets for the uncertain system $(G, \mathbf{\Delta})$, where $\mathbf{\Delta} \in \text{pwIQC}(\Psi, S)$ and $d \in \mathbf{D}_\Lambda$.

Theorem 3. Consider the uncertain system $(G, \mathbf{\Delta})$ defined in (1) with state x_G and output y such that $\mathbf{\Delta} \in \text{pwIQC}(\Psi, S)$ and the corresponding augmented system H defined in (4) with state x_H . If there exist $\tilde{P} \in \mathbb{S}_{++}^{n_G+n_y}$,

$\tilde{\tau}_1 \geq 0, \tilde{\tau}_2 \geq 0$, and $\tilde{\tau}_3 \geq 0$ such that

$$\text{blkdiag} \left(- \begin{bmatrix} A_H & B_{H1} & B_{H2} \end{bmatrix}^T \tilde{P} \begin{bmatrix} A_H & B_{H1} & B_{H2} \end{bmatrix}, 1 \right) - \tilde{\tau}_1 \text{blkdiag} \left(- \begin{bmatrix} I & 0 & 0 \end{bmatrix}^T \tilde{P} \begin{bmatrix} I & 0 & 0 \end{bmatrix}, 1 \right) \tag{15}$$

$$- \tilde{\tau}_2 \text{blkdiag} \left(\begin{bmatrix} C_{H1} & D_{H11} & D_{H12} \end{bmatrix}^T S \begin{bmatrix} C_{H1} & D_{H11} & D_{H12} \end{bmatrix}, 0 \right) - \tilde{\tau}_3 \text{blkdiag} \left(- \begin{bmatrix} 0 & 0 & I \end{bmatrix}^T \Lambda \begin{bmatrix} 0 & 0 & I \end{bmatrix}, 1 \right) \succcurlyeq 0, \tag{15}$$

then, for any $k \in \mathbb{N}_0$, $x_H^T(k) \tilde{P} x_H(k) \leq 1$ implies that $x_H^T(k+1) \tilde{P} x_H(k+1) \leq 1$ for all $\Delta \in \mathbf{\Delta}$ and $d(k) \in \mathcal{E}_\Lambda$.

Furthermore, if there exist $\tilde{Q} \in \mathbb{S}_{++}^{n_y}$, $\tilde{\tau}_4 \geq 0, \tilde{\tau}_5 \geq 0$, and $\tilde{\tau}_6 \geq 0$ such that

$$\text{blkdiag} \left(- \begin{bmatrix} C_{H2} & D_{H21} & D_{H22} \end{bmatrix}^T \tilde{Q} \begin{bmatrix} C_{H2} & D_{H21} & D_{H22} \end{bmatrix}, 1 \right) - \tilde{\tau}_4 \text{blkdiag} \left(- \begin{bmatrix} I & 0 & 0 \end{bmatrix}^T \tilde{P} \begin{bmatrix} I & 0 & 0 \end{bmatrix}, 1 \right) \tag{16}$$

$$- \tilde{\tau}_5 \text{blkdiag} \left(\begin{bmatrix} C_{H1} & D_{H11} & D_{H12} \end{bmatrix}^T S \begin{bmatrix} C_{H1} & D_{H11} & D_{H12} \end{bmatrix}, 0 \right) - \tilde{\tau}_6 \text{blkdiag} \left(- \begin{bmatrix} 0 & 0 & I \end{bmatrix}^T \Lambda \begin{bmatrix} 0 & 0 & I \end{bmatrix}, 1 \right) \succcurlyeq 0, \tag{16}$$

then, for any $k \in \mathbb{N}_0$, $x_H^T(k) \tilde{P} x_H(k) \leq 1$ implies that $y^T(k) \tilde{Q} y(k) \leq 1$ for all $\Delta \in \mathbf{\Delta}$ and $d(k) \in \mathcal{E}_\Lambda$.

Proof. Consider the quadratic functions

$$\tilde{\sigma}_0^{(1)}(x) = \begin{bmatrix} x^T & 1 \end{bmatrix} \text{blkdiag} \left(- \begin{bmatrix} A_H & B_{H1} & B_{H2} \end{bmatrix}^T \tilde{P} \begin{bmatrix} A_H & B_{H1} & B_{H2} \end{bmatrix}, 1 \right) \begin{bmatrix} x \\ 1 \end{bmatrix},$$

$$\tilde{\sigma}_0^{(2)}(x) = \begin{bmatrix} x^T & 1 \end{bmatrix} \text{blkdiag} \left(- \begin{bmatrix} C_{H2} & D_{H21} & D_{H22} \end{bmatrix}^T \tilde{Q} \begin{bmatrix} C_{H2} & D_{H21} & D_{H22} \end{bmatrix}, 1 \right) \begin{bmatrix} x \\ 1 \end{bmatrix},$$

$$\tilde{\sigma}_1(x) = \begin{bmatrix} x^T & 1 \end{bmatrix} \text{blkdiag} \left(- \begin{bmatrix} I & 0 & 0 \end{bmatrix}^T \tilde{P} \begin{bmatrix} I & 0 & 0 \end{bmatrix}, 1 \right) \begin{bmatrix} x \\ 1 \end{bmatrix},$$

$$\tilde{\sigma}_2(x) = \begin{bmatrix} x^T & 1 \end{bmatrix} \text{blkdiag} \left(\begin{bmatrix} C_{H1} & D_{H11} & D_{H12} \end{bmatrix}^T S \begin{bmatrix} C_{H1} & D_{H11} & D_{H12} \end{bmatrix}, 0 \right) \begin{bmatrix} x \\ 1 \end{bmatrix},$$

$$\tilde{\sigma}_3(x) = \begin{bmatrix} x^T & 1 \end{bmatrix} \text{blkdiag} \left(- \begin{bmatrix} 0 & 0 & I \end{bmatrix}^T \Lambda \begin{bmatrix} 0 & 0 & I \end{bmatrix}, 1 \right) \begin{bmatrix} x \\ 1 \end{bmatrix}.$$

Let $\xi(k) = (x_H(k), \vartheta(k), d(k))$. The following equivalences hold: $x_H^T(k+1) \tilde{P} x_H(k+1) \leq 1, x_H^T(k) \tilde{P} x_H(k) \leq 1, r^T(k) S r(k) \geq 0, d^T(k) \Lambda d(k) \leq 1$, and $y^T(k) \tilde{Q} y(k) \leq 1$ if and only if $\tilde{\sigma}_0^{(1)}(\xi(k)) \geq 0, \tilde{\sigma}_1(\xi(k)) \geq 0, \tilde{\sigma}_2(\xi(k)) \geq 0, \tilde{\sigma}_3(\xi(k)) \geq 0$, and $\tilde{\sigma}_0^{(2)}(\xi(k)) \geq 0$, respectively.

By the S-procedure, if (15) holds with $\tilde{P} \succ 0$ and $\tilde{\tau}_1, \tilde{\tau}_2$, and $\tilde{\tau}_3$ nonnegative, then $\tilde{\sigma}_0^{(1)}(\xi(k)) \geq 0$ whenever $\tilde{\sigma}_1(\xi(k)) \geq 0, \tilde{\sigma}_2(\xi(k)) \geq 0$, and $\tilde{\sigma}_3(\xi(k)) \geq 0$. Similarly, if (16) holds with $\tilde{P} \succ 0, \tilde{Q} \succ 0$, and $\tilde{\tau}_4, \tilde{\tau}_5$, and $\tilde{\tau}_6$ nonnegative, then $\tilde{\sigma}_0^{(2)}(\xi(k)) \geq 0$ whenever $\tilde{\sigma}_1(\xi(k)) \geq 0, \tilde{\sigma}_2(\xi(k)) \geq 0$, and $\tilde{\sigma}_3(\xi(k)) \geq 0$. To conclude, $\tilde{\sigma}_2(\xi(k)) \geq 0$ since $\mathbf{\Delta} \in \text{pwIQC}(\Psi, S), \tilde{\sigma}_3(\xi(k)) \geq 0$ since $d(k) \in \mathcal{E}_\Lambda$, and $\tilde{\sigma}_1(\xi(k)) \geq 0$ by assumption. ■

Corollary 1. Consider the uncertain system $(G, \mathbf{\Delta})$ defined in (1) with state x_G and output y such that $\mathbf{\Delta} \in \text{pwIQC}(\Psi, S)$ and the corresponding augmented system H defined in (4) with state x_H . Let \mathbf{D}_Λ be the set defined in (6). Then, the following hold.

- (1) If there exist $\tilde{P} \in \mathbb{S}_{++}^{n_G+n_\Psi}$, $\tilde{\tau}_1 \geq 0, \tilde{\tau}_2 \geq 0$, and $\tilde{\tau}_3 \geq 0$ such that (15) holds, then $x_G(0) \in \mathcal{E}_{\tilde{P}_{11}}$, that is, $x_H(0) \in \mathcal{E}_{\tilde{P}}$, implies that $x_G(k) \in \mathcal{E}_{\tilde{W}}$ and $x_H(k) \in \mathcal{E}_{\tilde{P}}$ for all $k \in \mathbb{N}_0, \Delta \in \mathbf{\Delta}$, and $d \in \mathbf{D}_\Lambda$, where $\tilde{W} = \tilde{P}_{11} - \tilde{P}_{12} \tilde{P}_{22}^{-1} \tilde{P}_{12}^T$.
- (2) If there exist $\tilde{P} \in \mathbb{S}_{++}^{n_G+n_\Psi}, \tilde{Q} \in \mathbb{S}_{++}^{n_y}$, and nonnegative $\tilde{\tau}_1, \dots, \tilde{\tau}_6$ such that (15) and (16) hold, then $x_G(0) \in \mathcal{E}_{\tilde{P}_{11}}$ implies that $y(k) \in \mathcal{E}_{\tilde{Q}}$ for all $k \in \mathbb{N}_0, \Delta \in \mathbf{\Delta}$, and $d \in \mathbf{D}_\Lambda$.

Proof. The result follows from a repeated application of Theorem 3, taking into account that \tilde{W} and \tilde{P} satisfy (10) for $\tau_3 = 1$ and $x_\Psi(0) = 0$. ■

Both (8) and (15) (respectively, (13) and (16)) are derived using the S-procedure. The left-hand side of (15) has a larger size and contains an extra term, whereas that of (8) is parameter dependent, which necessitates the imposition of (8) at

all $v_i \in V$ and the addition of condition (9). Thus, the number of constraints in Theorems 1 and 2 increases with p , the number of vertices of Γ . This increase is circumvented in Theorem 3 and Corollary 1.

Remark 5. The conditions in Theorem 3 clearly imply the robust uniform stability of the uncertain system (G, Δ) . Using a similar argument to the one used in Remark 1, it can be shown that if there exist $\tilde{P} \in \mathbb{S}_{++}^{n_G+n_\Psi}$, $\tilde{\tau}_1 \geq 0$, $\tilde{\tau}_2 \geq 0$, and $\tilde{\tau}_3 \geq 0$ such that (15) holds, then the system is robustly uniformly stable,³¹ that is, $\|x_G(k)\|_2 \leq c\|x_G(0)\|_2$ for any $x_G(0) \in \mathbb{R}^{n_G}$, $k \in \mathbb{N}_0$, $\Delta \in \Delta$, and $d \equiv 0$, with $c = \sqrt{\text{cond}(\tilde{P})}$. Furthermore, if the solutions \tilde{P} and $\tilde{\tau}_2 S$ are such that (11) holds with strict inequality when P and τ_2 are substituted with \tilde{P} and $\tilde{\tau}_2$, respectively, then the uncertain system is robustly asymptotically stable.^{5(Theorem 1)}

Remark 6. It is possible to incorporate local pointwise IQCs³³ into the conditions of Theorem 3. Similarly to Remark 3, two approaches can be used to ensure that the elements of $\varphi(k)$ are restricted to their local intervals. The first approach relies on the S-procedure. Specifically, in this approach, for $j = 1, \dots, n_\varphi$, we define four quadratic functions $\bar{\sigma}_0(x)$, $\bar{\sigma}_1(x)$, $\bar{\sigma}_2(x)$, and $\bar{\sigma}_3(x)$ such that, for $\xi(k) = (x_H(k), \vartheta(k), d(k))$, the inequalities $\bar{\sigma}_0(\xi(k)) \geq 0$, $\bar{\sigma}_1(\xi(k)) \geq 0$, $\bar{\sigma}_2(\xi(k)) \geq 0$, and $\bar{\sigma}_3(\xi(k)) \geq 0$ are equivalent to $|\varphi_j(k)| \leq \bar{\varphi}_j$, $x_H^T(k) P x_H(k) \leq 1$, $r^T(k) S_{\text{loc},j} r(k) \geq 0$, and $d^T(k) \Lambda d(k) \leq 1$, respectively. Then, we derive a matrix inequality similar to (15) using Lemma 1. Hence, given the bounds on the components $\varphi_j(k)$ of $\varphi(k)$, these inequalities can be enforced alongside the inequalities of Theorem 3, where S is substituted with S_{loc} . The second approach may be applied when $D_{G11} = 0$ and consists of enforcing the conditions of Theorem 3 alongside inequality (12) for $j = 1, \dots, n_\varphi$, where P is substituted with \tilde{P} and $\bar{d}_j = \max_{d(k) \in \mathcal{E}_\Lambda} (D_{G12}^{(j)} d(k))$.

Remark 7. In Theorems 1 and 2, the size of the left-hand sides of inequalities (8) and (13), which are imposed at each vertex $v_i \in V$, is $(n_G + n_\Psi + n_\vartheta + 1) \times (n_G + n_\Psi + n_\vartheta + 1)$, and the size of the left-hand sides of the added constraints (9) and (14) is $n_d \times n_d$. In Theorem 3 and Corollary 1, the size of the left-hand sides of (15) and (16) is $(n_G + n_\Psi + n_\vartheta + n_d + 1) \times (n_G + n_\Psi + n_\vartheta + n_d + 1)$. In both cases, the decision variables appearing in the formulated optimization problems are the same, namely, $(P, Q, \tau_1, \tau_2, \tau_4, \tau_5)$ and $(\tilde{P}, \tilde{Q}, \tilde{\tau}_1, \tilde{\tau}_2, \tilde{\tau}_4, \tilde{\tau}_5)$, and the nonlinearities can be handled in the same way, that is, via sequentially solving for the state and output bounding ellipsoids while gridding over one parameter in the first step or simultaneously solving for both ellipsoids while resorting to double gridding. In the case of Theorem 3 and Corollary 1, there are additional nonnegative scalar variables $\tilde{\tau}_3$ and $\tilde{\tau}_6$ that appear linearly in (15) and (16), respectively.

The size of the optimization problems formulated in Section 4 may become prohibitive for a large p . Nonetheless, modern convex optimization tools, such as Yalmip³⁵ and MOSEK,³⁶ are able to efficiently handle reasonably large problems. Moreover, the results derived in this section can still be applied even when $d \in \mathbf{D}_\Gamma$ by using ellipsoidal approximations of Γ , for example, the maximum/minimum volume inscribed/covering ellipsoid centered at the origin. The following example gives an idea of the complexity of the results when applied to real systems.

Example 1. We compute bounding sets for the LPV path-following controller designed in the article³⁷ for a small, fixed-wing, unmanned aircraft system. Namely, ellipsoids are computed in which the state of the LPV controller and its output (control input to the plant) lie for all time-steps given bounded measurements from the plant (input to the controller). The reported computations are carried out in MATLAB 9.5 on a Dell desktop with Intel Xeon E-2224G, 3.5 GHz processor, and 32 GB of RAM running Windows 10 Enterprise. The parser and solver used are Yalmip and MOSEK, respectively. The LPV controller, that is, the uncertain system (G, Δ) in this case, is well-posed (in fact, robustly stable) and has $n_G = 16$ state variables, $n_d = 10$ inputs, and $n_y = 4$ outputs. Using flight-test data, a tight hyper-rectangle is determined in which $d(k)$ resides for all $k \in \mathbb{N}_0$. The constructed hyper-rectangle Γ is relaxed/enlarged to become symmetric such that (8) and (13) can be imposed at $2^{n_d-1} = 2^9$ vertices instead of $2^{n_d} = 2^{10}$ vertices. For comparison, the minimum volume ellipsoid \mathcal{E}_Λ centered at the origin and covering Γ is also computed to apply the results of Section 5. In LFT form, there are $n_\varphi = n_\vartheta = 7$ copies of the scheduling parameter $\delta(k)$. Rate bounds can be computed on $\delta(k)$, and so Δ is viewed as the set of rate-bounded, static LTV uncertainty operators; see Proposition 6. As explained in Section 6, an augmented system G_e and uncertainty set Δ_e are formed in this case such that $\Delta_e \in \text{pwIQC}(\Psi, S)$, and the analysis is performed on (G_e, Δ_e) . The dynamic IQC filter Ψ utilized for the analysis has $n_\Psi = 28$ state variables, and so the dimension of the state vector of the augmented system is $n_H = n_G + n_\Psi = 44$. The IQC variables in S are $X \in \mathbb{S}_+^{21}$, $\bar{X} \in \mathbb{S}_+^{14}$, and skew-symmetric matrices Y and \bar{Y} in $\mathbb{R}^{21 \times 21}$ and $\mathbb{R}^{14 \times 14}$, respectively. For the above described problem setup, solving one instance of the SDP for finding the minimum

volume state bounding ellipsoid, that is, for a given $\tau_1/\tilde{\tau}_1$ value, takes on average 2618.9 s when $d \in \mathbf{D}_\Gamma$ and 5.9 s when $d \in \mathbf{D}_\Lambda$, respectively. Solving for the output bounding ellipsoid for a given state bounding ellipsoid is a convex problem, that is, needs to be solved only once, and takes on average 386.3 s when $d \in \mathbf{D}_\Gamma$ and 0.9 s when $d \in \mathbf{D}_\Lambda$, respectively.

6 | EXAMPLES OF POINTWISE INTEGRAL QUADRATIC CONSTRAINTS

This section gives examples of uncertainty sets that admit pointwise IQC characterizations that can be extracted from the ones presented in References 1,3,38-40.

Proposition 1 (38). *Let Δ be the set of static LTI operators Δ that represent the multiplication in the time-domain by an uncertain scalar δ , that is, $\vartheta = \Delta(\varphi)$ means that $\vartheta(k) = \delta I_{n_\varphi} \varphi(k)$, where $|\delta| \leq \alpha$, for all $k \in \mathbb{N}_0$. Then, $\Delta \in \text{pwIQC}(\Psi, S)$, where*

$$\Psi(z) = \begin{bmatrix} \mathcal{B}(z) & 0 \\ 0 & \mathcal{B}(z) \end{bmatrix} \otimes I_{n_\varphi}, \quad S = \begin{bmatrix} \alpha^2 X & Y \\ Y^T & -X \end{bmatrix}, \quad (17)$$

$X = X^T \in \mathbb{S}_+^{n_B \times n_\varphi}$, $Y = -Y^T$ in $\mathbb{R}^{(n_B \times n_\varphi) \times (n_B \times n_\varphi)}$, and $\mathcal{B} \in \mathbb{RH}_\infty^{n_B \times 1}$.

Proof. The proof is an adaptation of its continuous-time counterpart.³⁸ For $i = 1, \dots, n_B$ and $j = 1, \dots, n_\varphi$, define signals $\mu_{i,j}$ and $\eta_{i,j}$ in ℓ_{2e}^1 such that

$$\begin{bmatrix} \mu_{1,j} \\ \vdots \\ \mu_{n_B,j} \end{bmatrix} = \mathcal{B} \varphi_j, \quad \begin{bmatrix} \eta_{1,j} \\ \vdots \\ \eta_{n_B,j} \end{bmatrix} = \mathcal{B} \vartheta_j,$$

Let $\tilde{\mu}_i = (\mu_{i,1}, \dots, \mu_{i,n_\varphi})$ and $\tilde{\eta}_i = (\eta_{i,1}, \dots, \eta_{i,n_\varphi})$ for $i = 1, \dots, n_B$, and define $\hat{\mu} = (\tilde{\mu}_1, \dots, \tilde{\mu}_{n_B})$ and $\hat{\eta} = (\tilde{\eta}_1, \dots, \tilde{\eta}_{n_B})$. It can be seen that $r = \Psi \begin{bmatrix} \varphi \\ \vartheta \end{bmatrix} = \begin{bmatrix} \hat{\mu} \\ \hat{\eta} \end{bmatrix}$. Since $\vartheta(k) = \delta \varphi(k)$ for all $k \in \mathbb{N}_0$, it follows by linearity of \mathcal{B} that $\eta_{i,j} = \delta \mu_{i,j}$ for all i and j . Thus, $\hat{\eta} = \delta \hat{\mu}$ and

$$r^T(k) S r(k) = \begin{bmatrix} \hat{\mu}^T(k) & \hat{\eta}^T(k) \end{bmatrix} \begin{bmatrix} \alpha^2 X & Y \\ Y^T & -X \end{bmatrix} \begin{bmatrix} \hat{\mu}(k) \\ \hat{\eta}(k) \end{bmatrix} = (\alpha^2 - \delta^2) \hat{\mu}^T(k) X \hat{\mu}(k) \geq 0,$$

for all $k \in \mathbb{N}_0$, which concludes the proof. ■

Proposition 2 (38). *Let Δ be the set of static LTV operators Δ that represent the multiplication in the time-domain by a time-varying scalar $\delta(k)$, that is, $\vartheta = \Delta(\varphi)$ means that $\vartheta(k) = \delta(k) I_{n_\varphi} \varphi(k)$, where $|\delta(k)| \leq \alpha$, for all $k \in \mathbb{N}_0$. Then, $\Delta \in \text{pwIQC}(\Psi, S)$, where*

$$\Psi(z) = \begin{bmatrix} I_{n_\varphi} & 0 \\ 0 & I_{n_\varphi} \end{bmatrix}, \quad S = \begin{bmatrix} \alpha^2 X & Y \\ Y^T & -X \end{bmatrix}, \quad (18)$$

$X = X^T \in \mathbb{S}_+^{n_\varphi}$, and $Y = -Y^T$ in $\mathbb{R}^{n_\varphi \times n_\varphi}$.

Proof. The proof is analogous to its continuous-time counterpart.³⁸(Appendix B) ■

Proposition 3 (38). *Consider the functions $\phi_i : \mathbb{R} \times \mathbb{R} \mapsto \mathbb{R}$ satisfying $(\phi_i(x, k) - \alpha_i x)(\beta_i x - \phi_i(x, k)) \geq 0$ and $\phi_i(0, k) = 0$, where $\alpha_i \leq \beta_i$, for all $x \in \mathbb{R}$, $k \in \mathbb{N}_0$, and $i = 1, \dots, n_\varphi$. Let Δ be the set of time-varying, memoryless, and sector-bounded nonlinearities $\Delta = \text{diag}(\tilde{\Delta}_1, \dots, \tilde{\Delta}_{n_\varphi})$ such that $\vartheta = \Delta(\varphi)$ means that $\vartheta_i(k) = (\tilde{\Delta}_i(\varphi_i))(k) = \phi_i(\varphi_i(k), k)$ for all $k \in \mathbb{N}_0$ and $i = 1, \dots, n_\varphi$. Then, the following statements hold.*

(i) The set $\Delta \in \text{pwIQC}(\Psi, S)$, where

$$\Psi(z) = \begin{bmatrix} -\text{diag}(\alpha) & I_{n_\varphi} \\ \text{diag}(\beta) & -I_{n_\varphi} \end{bmatrix}, \quad S = \begin{bmatrix} 0 & S_{12} \\ S_{12}^T & 0 \end{bmatrix}, \quad (19)$$

$S_{12} = \text{diag}(S_1, \dots, S_{n_\varphi})$ with $S_i \geq 0$ for $i = 1, \dots, n_\varphi$, $\alpha = (\alpha_1, \dots, \alpha_{n_\varphi})$, and $\beta = (\beta_1, \dots, \beta_{n_\varphi})$.

(ii) The set $\Delta \in \text{pwIQC}(\Psi, S)$, where

$$\Psi(z) = \begin{bmatrix} I_{n_\varphi} & 0 \\ 0 & I_{n_\varphi} \end{bmatrix}, \quad S \in \mathbf{S}, \quad (20)$$

$$\mathbf{S} = \left\{ S \in \mathbb{S}^{2n_\varphi} \mid \begin{bmatrix} I_{n_\varphi} \\ \text{diag}(\delta) \end{bmatrix}^T S \begin{bmatrix} I_{n_\varphi} \\ \text{diag}(\delta) \end{bmatrix} \geq 0 \text{ for all } \delta \in \mathbb{R}^{n_\varphi} \text{ such that } \delta_i \in [\alpha_i, \beta_i] \text{ for } i = 1, \dots, n_\varphi \right\}.$$

Proof. The proofs of statements (i) and (ii) are analogous to their continuous-time counterparts.³⁸(Appendix B) ■
For $n_\varphi = 1$, the factors in (19) give

$$\Pi = \Psi^T S \Psi = S_1 \begin{bmatrix} -2\alpha_1\beta_1 & \alpha_1 + \beta_1 \\ \alpha_1 + \beta_1 & -2 \end{bmatrix} = \tilde{\Psi}^T \tilde{S} \tilde{\Psi},$$

$$\tilde{\Psi} = \begin{bmatrix} 1 & 0 \\ 0 & 1 \end{bmatrix}, \quad \tilde{S} = S_1 \begin{bmatrix} -2\alpha_1\beta_1 & \alpha_1 + \beta_1 \\ \alpha_1 + \beta_1 & -2 \end{bmatrix}.$$

In the above, the notation is simplified and the dependence on z is dropped since Ψ and $\tilde{\Psi}$ are static filters. For $n_\varphi = 1$, Proposition 3 in Reference 27 states that a set Δ similar to the one defined in Proposition 3 here satisfies $\Delta \in \text{pwIQC}(\tilde{\Psi}, \tilde{S})$. Thus, the factors in (19) generalize the ones in Reference 27 to the case $n_\varphi \geq 1$. Moreover, the pointwise IQC characterization of Δ in statement (i) is a special case of that in statement (ii). We illustrate this for $n_\varphi = 1$ for simplicity. As argued above, statement (i) means that $\Delta \in \text{pwIQC}(\tilde{\Psi}, \tilde{S})$. Since $\tilde{\Psi}$ has the form of Ψ in (20), it is only needed to show that $\tilde{S} \in \mathbf{S}$. Namely,

$$\begin{bmatrix} 1 & \delta_1 \end{bmatrix} \tilde{S} \begin{bmatrix} 1 \\ \delta_1 \end{bmatrix} = 2S_1(\delta_1 - \alpha_1)(\beta_1 - \delta_1) \geq 0,$$

for all $\delta_1 \in [\alpha_1, \beta_1]$, since $S_1 \geq 0$.

The set \mathbf{S} is defined by an infinite number of LMI constraints. For implementation, the Polya relaxation technique³⁸(Section 5.2.2) is used herein to find sufficient conditions for S to be in \mathbf{S} that are defined by a finite number of LMI constraints.

Proposition 4 (1). *Let Δ be the set of static LTV operators Δ that represent the multiplication in the time-domain by a time-varying matrix $L(k)$ such that $L(k) \in \mathcal{L}$ for all $k \in \mathbb{N}_0$, where \mathcal{L} is a polytope of matrices with N vertices L_1, \dots, L_N . In other words, $\vartheta = \Delta(\varphi)$ means that $\vartheta(k) = L(k)\varphi(k)$, where $L(k) \in \mathcal{L}$, for all $k \in \mathbb{N}_0$. Then, $\Delta \in \text{pwIQC}(\Psi, S)$, where*

$$\Psi(z) = \begin{bmatrix} I_{n_\varphi} & 0 \\ 0 & I_{n_\vartheta} \end{bmatrix}, \quad S = \begin{bmatrix} X & F \\ F^T & R \end{bmatrix}, \quad (21)$$

$X \in \mathbb{S}^{n_\varphi}$, $R < 0$, and $X + FL_i + L_i^T F^T + L_i^T R L_i \geq 0$ for $i = 1, \dots, N$.

Proof. The proof is analogous to its continuous-time counterpart.¹ ■

Proposition 5 (3, Section 5). Let Δ be the set of operators Δ that represent uncertain time-varying time-delays in the time-domain, namely, $\vartheta = \Delta(\varphi)$ means that $\vartheta(k) = \varphi(k - \tau(k)) - \varphi(k)$, where $\tau : \mathbb{N}_0 \mapsto \mathbb{N}_0$ is the time-delay function defined such that $0 \leq \tau(k) \leq \tau_{\max}$, for all $k \in \mathbb{N}_0$. Then, $\Delta \in \text{pwIQC}(\Psi, S)$, where the realization of Ψ is given by

$$\left[\begin{array}{c|cc} A_\Psi & B_{\Psi_1} & B_{\Psi_2} \\ \hline C_\Psi & D_{\Psi_1} & D_{\Psi_2} \end{array} \right] = \left[\begin{array}{ccc|cc} \begin{bmatrix} 0 & I_{n_\varphi} & 0 & 0 \\ \vdots & \ddots & \ddots & \vdots \\ \vdots & \ddots & \ddots & I_{n_\varphi} \\ 0 & \dots & \dots & 0 \end{bmatrix} & \begin{bmatrix} 0 \\ 0 \\ 0 \\ I_{n_\varphi} \end{bmatrix} & \begin{bmatrix} 0 \\ \vdots \\ \vdots \\ 0 \end{bmatrix} \\ \hline \begin{bmatrix} I_{n_\varphi} & -I_{n_\varphi} & 0 & 0 \\ 0 & \ddots & \ddots & 0 \\ \vdots & \ddots & \ddots & -I_{n_\varphi} \\ \vdots & \ddots & \ddots & I_{n_\varphi} \\ 0 & \dots & \dots & 0 \end{bmatrix} & \begin{bmatrix} 0 \\ \vdots \\ 0 \\ -I_{n_\varphi} \\ 0 \end{bmatrix} & \begin{bmatrix} 0 \\ \vdots \\ \vdots \\ 0 \\ I_{n_\varphi} \end{bmatrix} \end{array} \right], \tag{22}$$

with $n_\Psi = \tau_{\max}n_\varphi$, $n_r = n_\varphi(\tau_{\max} + 1)$, and $S \succcurlyeq S_i$ for $i = 0, \dots, \tau_{\max}$, where $S_i = \text{blkdiag}(\bar{X}_i, -X)$, $X = X^T \in \mathbb{S}_+^{n_\varphi}$, $\bar{X}_i = \text{blkdiag}(0_{(\tau_{\max}-i) \times (\tau_{\max}-i)}, \mathbf{1}_i) \otimes X$, and $\mathbf{1}_i$ is the $i \times i$ all ones matrix.

The final example of an uncertainty set Δ that can be characterized by a pointwise IQC is the set of rate-bounded static LTV operators that represent the multiplication in the time-domain by a rate-bounded time-varying scalar. To perform IQC-based analysis on (G, Δ) in this case, an augmented system $G_e = \begin{bmatrix} G_{11} & 0 & G_{12} \\ G_{21} & 0 & G_{22} \end{bmatrix}$ and uncertainty set Δ_e are formed such that Δ_e satisfies an appropriate IQC, and the analysis is performed on the system (G_e, Δ_e) .^{39,40} Proposition 6 gives the set Δ_e and corresponding factors (Ψ, S) and shows that $\Delta_e \in \text{pwIQC}(\Psi, S)$.

Proposition 6 (39,40). Let Δ be the set of rate-bounded static LTV operators Δ that represent the multiplication in the time-domain by a rate-bounded time-varying scalar $\delta(k)$, that is, $\vartheta = \Delta(\varphi)$ means that $\vartheta(k) = \delta(k)I_{n_\varphi}\varphi(k)$, where $|\delta(k)| \leq \alpha$ and $|\delta(k + 1) - \delta(k)| \leq \beta$, for all $k \in \mathbb{N}_0$. Define Δ_e as the set of operators Δ_e such that

$$\begin{bmatrix} \vartheta_1 \\ \vartheta_2 \end{bmatrix} = \Delta_e(\varphi) = \begin{bmatrix} \Delta(\varphi) \\ (Z^* \Delta Z - \Delta)\mu \end{bmatrix}, \quad \Delta \in \Delta,$$

where the time-shift operator Z satisfies $((Z^* \Delta Z)\mu)(k) = \delta(k + 1)\mu(k)$ for all $k \in \mathbb{N}_0$ and $\Delta \in \Delta$, and μ is the output of a stable LTI system with realization $(\hat{A}_\Psi \otimes I_{n_\varphi}, \hat{B}_\Psi \otimes I_{n_\varphi}, \hat{A}_\Psi \otimes I_{n_\varphi}, \hat{B}_\Psi \otimes I_{n_\varphi})$ driven by φ and starting from zero initial conditions, with $\hat{A}_\Psi \in \mathbb{R}^{\hat{n} \times \hat{n}}$ and $\hat{B}_\Psi \in \mathbb{R}^{\hat{n} \times 1}$ for some positive integer \hat{n} . Then, $\Delta_e \in \text{pwIQC}(\Psi, S)$, where the realization of Ψ is given by

$$\left[\begin{array}{c|cc} A_\Psi & B_{\Psi_1} & B_{\Psi_2} \\ \hline C_\Psi & D_{\Psi_1} & D_{\Psi_2} \end{array} \right] = \left[\begin{array}{ccc|cc} \begin{bmatrix} \hat{A}_\Psi & 0 \\ 0 & \hat{A}_\Psi \end{bmatrix} & \begin{bmatrix} \hat{B}_\Psi \\ 0 \end{bmatrix} & \begin{bmatrix} 0 & 0 \\ \hat{B}_\Psi & I_{\hat{n}} \end{bmatrix} \\ \hline \begin{bmatrix} \hat{C}_\Psi & 0 \\ \hat{A}_\Psi & 0 \\ 0 & \hat{C}_\Psi \\ 0 & 0 \end{bmatrix} & \begin{bmatrix} \hat{D}_\Psi \\ \hat{B}_\Psi \\ 0 \\ 0 \end{bmatrix} & \begin{bmatrix} 0 & 0 \\ 0 & 0 \\ \hat{D}_\Psi & 0 \\ 0 & I_{\hat{n}} \end{bmatrix} \end{array} \right] \otimes I_{n_\varphi}, \tag{23}$$

with $\hat{C}_\Psi \in \mathbb{R}^{n_B \times \hat{n}}$ and $\hat{D}_\Psi \in \mathbb{R}^{n_B \times 1}$ for some positive integer n_B , and

$$S = \begin{bmatrix} \alpha^2 X & 0 & Y & 0 \\ 0 & \beta^2 \bar{X} & 0 & \bar{Y} \\ Y^T & 0 & -X & 0 \\ 0 & \bar{Y}^T & 0 & -\bar{X} \end{bmatrix}, \quad (24)$$

where $X = X^T \in \mathbb{S}_+^{n_B \times n_\varphi}$, $\bar{X} = \bar{X}^T \in \mathbb{S}_+^{\hat{n} \times n_\varphi}$, $Y = -Y^T$ in $\mathbb{R}^{(n_B \times n_\varphi) \times (n_B \times n_\varphi)}$, and $\bar{Y} = -\bar{Y}^T$ in $\mathbb{R}^{(\hat{n} \times n_\varphi) \times (\hat{n} \times n_\varphi)}$.

Proof. The proof is an adaptation of its continuous-time counterpart.^{39,40} The equations for ϑ_1 and ϑ_2 are given by $\eta_1(0) = 0$, $\vartheta_1(k) = \delta(k)\varphi(k)$, $\vartheta_2(k) = (\delta(k+1) - \delta(k))\mu(k)$,

$$\begin{aligned} \eta_1(k+1) &= (\hat{A}_\Psi \otimes I_{n_\varphi})\eta_1(k) + (\hat{B}_\Psi \otimes I_{n_\varphi})\varphi(k), \\ \mu(k) &= (\hat{A}_\Psi \otimes I_{n_\varphi})\eta_1(k) + (\hat{B}_\Psi \otimes I_{n_\varphi})\varphi(k) = \eta_1(k+1), \end{aligned}$$

for all $k \in \mathbb{N}_0$. Ψ maps $(\varphi, (\vartheta_1, \vartheta_2))$ to $r = (r_1, r_2, r_3, r_4)$. Let the state vector of Ψ be partitioned as $x_\Psi(k) = (\xi_1(k), \xi_2(k))$. The filter equations are given by $\xi_1(0) = 0$, $\xi_2(0) = 0$, and

$$\begin{aligned} \xi_1(k+1) &= (\hat{A}_\Psi \otimes I_{n_\varphi})\xi_1(k) + (\hat{B}_\Psi \otimes I_{n_\varphi})\varphi(k), \\ \xi_2(k+1) &= (\hat{A}_\Psi \otimes I_{n_\varphi})\xi_2(k) + (\hat{B}_\Psi \otimes I_{n_\varphi})\vartheta_1(k) + \vartheta_2(k), \\ r_1(k) &= (\hat{C}_\Psi \otimes I_{n_\varphi})\xi_1(k) + (\hat{D}_\Psi \otimes I_{n_\varphi})\varphi(k), \\ r_2(k) &= (\hat{A}_\Psi \otimes I_{n_\varphi})\xi_1(k) + (\hat{B}_\Psi \otimes I_{n_\varphi})\varphi(k) = \xi_1(k+1), \\ r_3(k) &= (\hat{C}_\Psi \otimes I_{n_\varphi})\xi_2(k) + (\hat{D}_\Psi \otimes I_{n_\varphi})\vartheta_1(k), \\ r_4(k) &= \vartheta_2(k) = (\delta(k+1) - \delta(k))\eta_1(k+1), \end{aligned}$$

for all $k \in \mathbb{N}_0$. Since $\eta_1(0) = \xi_1(0) = 0$, then $\eta_1(k) = \xi_1(k)$ and $r_4(k) = (\delta(k+1) - \delta(k))r_2(k)$ for all $k \in \mathbb{N}_0$. Moreover,

$$\xi_2(k+1) - \delta(k+1)\xi_1(k+1) = (\hat{A}_\Psi \otimes I_{n_\varphi})(\xi_2(k) - \delta(k)\xi_1(k)),$$

for all $k \in \mathbb{N}_0$. Since $\xi_2(0) = \xi_1(0) = 0$, it follows that $\xi_2(k) = \delta(k)\xi_1(k)$ and $r_3(k) = \delta(k)r_1(k)$ for all $k \in \mathbb{N}_0$. Since $Y = -Y^T$ and $\bar{Y} = -\bar{Y}^T$, $r^T(k)Sr(k)$ can be expanded as

$$r^T(k)Sr(k) = (\alpha^2 - \delta(k)^2)r_1^T(k)Xr_1(k) + (\beta^2 - (\delta(k+1) - \delta(k))^2)r_2^T(k)\bar{X}r_2(k),$$

which is nonnegative for all $k \in \mathbb{N}_0$, since $X \succeq 0$, $\bar{X} \succeq 0$, $|\delta(k)| \leq \alpha$, and $|\delta(k+1) - \delta(k)| \leq \beta$. ■

Remark 8. In Propositions 1, 2, and 6, the number of decision variables in the symmetric matrix S can be reduced by using an equivalent parametrization of S . Specifically, in Propositions 1 and 2, S can be parametrized as

$$S = \begin{bmatrix} \alpha I & -I \\ \alpha I & I \end{bmatrix}^T \begin{bmatrix} 0 & Y^T \\ Y & 0 \end{bmatrix} \begin{bmatrix} \alpha I & -I \\ \alpha I & I \end{bmatrix},$$

where $Y + Y^T \succeq 0$, while, in Proposition 6, S can be parametrized as

$$S = \begin{bmatrix} \alpha I & 0 & -I & 0 \\ 0 & \beta I & 0 & -I \\ \alpha I & 0 & I & 0 \\ 0 & \beta I & 0 & I \end{bmatrix}^T \begin{bmatrix} 0 & 0 & Y^T & 0 \\ 0 & 0 & 0 & \bar{Y}^T \\ Y & 0 & 0 & 0 \\ 0 & \bar{Y} & 0 & 0 \end{bmatrix} \begin{bmatrix} \alpha I & 0 & -I & 0 \\ 0 & \beta I & 0 & -I \\ \alpha I & 0 & I & 0 \\ 0 & \beta I & 0 & I \end{bmatrix},$$

where $Y + Y^T \succeq 0$ and $\bar{Y} + \bar{Y}^T \succeq 0$.

7 | ILLUSTRATIVE EXAMPLE

In this section, the proposed results are applied to a simplified model of an active automobile suspension system. The system under consideration appears in the book,⁴¹ and its state-space model is given by

$$\dot{q}(t) = A_c q(t) + B_{c,u} u(t) + B_{c,w} w(t),$$

where $q(t)$, $u(t)$, and $w(t)$ are the state, control input, and disturbance vectors at time $t \geq 0$, and

$$A_c = \begin{bmatrix} 0 & 0 & 1 & 0 \\ 0 & 0 & 0 & 1 \\ -\frac{k_{s1}}{M} & \frac{k_{s1}}{M} & -\frac{b_1}{M} & \frac{b_1}{M} \\ \frac{k_{s1}}{m} & -\frac{k_{s1}+k_{s2}}{m} & \frac{b_1}{m} & -\frac{b_1+b_2}{m} \end{bmatrix}, \quad B_{c,u} = \begin{bmatrix} 0 \\ 0 \\ \frac{1}{M} \\ -\frac{1}{m} \end{bmatrix}, \quad B_{c,w} = \begin{bmatrix} 0 & 0 \\ 0 & 0 \\ 0 & 0 \\ \frac{k_{s2}}{m} & \frac{b_2}{m} \end{bmatrix}.$$

The values considered for the parameters are $M = 300$ kg, $m = 50$ kg, $k_{s2} = 30,000$ N/m, $b_1 = 600$ N/(m/s), and $b_2 = 1000$ N/(m/s). k_{s1} is an uncertain parameter defined as $k_{s1} = (1 + c\delta_1) \bar{k}_{s1}$, where $c = 0.2$, $\delta_1 \in [-1, 1]$, and $\bar{k}_{s1} = 3000$ N/m. The disturbance vector $w(t) = (z_R(t), \dot{z}_R(t))$, where $z_R(t)$ is the roadway profile with respect to some nominal height. The system equations are discretized using the Euler method with a sampling time $T = 0.01$ s, which preserves the affine dependence of the state-space matrices on δ_1 . The resulting discrete-time uncertain system model is given by

$$\bar{q}(k+1) = A_d(\delta_1) \bar{q}(k) + B_{d,u} \bar{u}(k) + B_{d,w} d(k),$$

where $\bar{q}(k) = q(kT)$ and $\bar{u}(k) = u(kT)$ for all $k \in \mathbb{N}_0$. For an appropriately defined $B_{d,w}$, we let $d(k) = (z_R(kT), dz_R(kT))$, where $dz_R(kT) = \dot{z}_R(kT)T$. A robust state feedback controller gain K is designed for the above discrete-time polytopic system using the method in the Reference 42. The applied input to the system is the summation of the control law $K\bar{q}(k)$ and a nonlinear uncertainty term $\phi(K\bar{q}(k))$, that is, $\bar{u}(k) = K\bar{q}(k) + \phi(K\bar{q}(k))$ for all $k \in \mathbb{N}_0$. $\phi : \mathbb{R} \rightarrow \mathbb{R}$ represents a time-invariant, memoryless, sector-bounded nonlinearity that satisfies $\phi(0) = 0$ and $(\phi(x) - \alpha x)(\beta x - \phi(x)) \geq 0$ for all $x \in \mathbb{R}$ with $\alpha = -0.1$ and $\beta = 0.15$. ϕ belongs to the set $\Delta_{SBN} \in \text{pwIQC}(\Psi_{SBN}, S_{SBN})$, where Ψ_{SBN} and S_{SBN} are defined in (20). Applying the input $\bar{u}(k)$, the following closed-loop system equation is obtained:

$$\bar{q}(k+1) = (A_d(\delta_1) + B_{d,u}K) \bar{q}(k) + B_{d,u}\phi(K\bar{q}(k)) + B_{d,w}d(k),$$

for all $k \in \mathbb{N}_0$. The outputs of interest are given by

$$y(k) = \begin{bmatrix} y_1(k) \\ y_2(k) \end{bmatrix} = C_d(\delta_1) \bar{q}(k) + D_{d,w}d(k) = \begin{bmatrix} -k_{s1} & k_{s1} & 0 & 0 \\ 0 & -k_{s2} & 0 & 0 \end{bmatrix} \bar{q}(k) + \begin{bmatrix} 0 & 0 \\ k_{s2} & 0 \end{bmatrix} d(k),$$

for all $k \in \mathbb{N}_0$. The outputs relate to the spring forces in the suspension system as follows: $F_{k_{s1}} = y_1 + Mg$ and $F_{k_{s2}} = y_2 + (M + m)g$, where g is the gravitational constant. Next, the equations of the formulated discrete-time uncertain system are

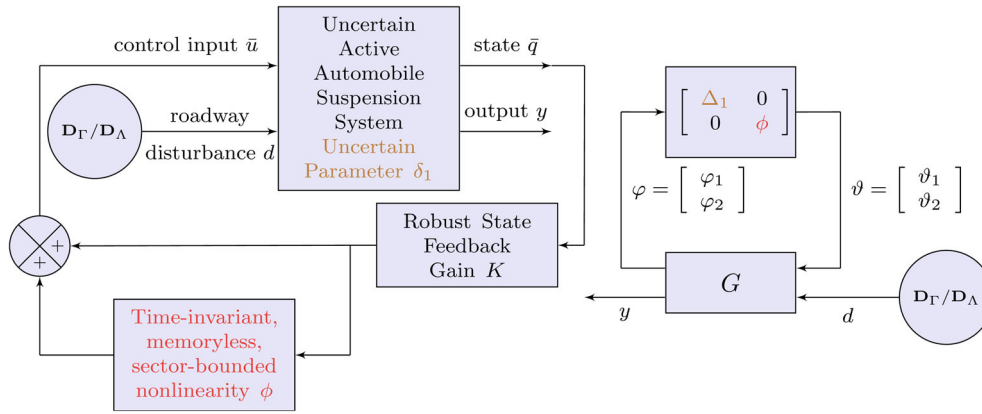


FIGURE 2 Schematic diagram (left) and equivalent LFT representation (right) of the uncertain system (G, Δ) analyzed in the illustrative example of Section 7.

expressed in LFT form as in (1). In the obtained LFT system (G, Δ) ,

$$\Delta = \begin{bmatrix} \Delta_1 & 0 \\ 0 & \phi \end{bmatrix}, \quad \vartheta = \begin{bmatrix} \vartheta_1 \\ \vartheta_2 \end{bmatrix} = \Delta(\varphi) = \Delta \left(\begin{bmatrix} \varphi_1 \\ \varphi_2 \end{bmatrix} \right) = \begin{bmatrix} \Delta_1(\varphi_1) \\ \phi(\varphi_2) \end{bmatrix},$$

where $\vartheta_1(k) = \Delta_1(\varphi_1(k)) = \delta_1 I_1 \varphi_1(k)$, with $\delta_1 \in [-1, 1]$, for all $k \in \mathbb{N}_0$. That is, $\Delta_1 \in \mathbf{\Delta}_{\text{SLTI}}$, where $\mathbf{\Delta}_{\text{SLTI}}$ is the set defined in Proposition 1 satisfying $\mathbf{\Delta}_{\text{SLTI}} \in \text{pwIQC}(\Psi_{\text{SLTI}}, S_{\text{SLTI}})$ with $\Psi_{\text{SLTI}}(z)$ and S_{SLTI} defined in (17). To construct $\Psi_{\text{SLTI}}(z)$, the basis transfer function matrix $\mathcal{B}(z) = \begin{bmatrix} 1 & \frac{1}{(z-\lambda)} & \frac{1}{(z-\lambda)^2} \end{bmatrix}^T$ is used with $\lambda = 0.8$. Thus, $\Delta \in \mathbf{\Delta}$, where

$$\mathbf{\Delta} = \{ \Delta = \text{blkdiag}(\Delta_1, \phi) \mid \Delta_1 \in \mathbf{\Delta}_{\text{SLTI}}, \phi \in \mathbf{\Delta}_{\text{SBN}} \}.$$

The set $\mathbf{\Delta} \in \text{pwIQC}(\Psi, S)$, where $\Psi(z)$ and S are obtained by block-diagonal augmentation of the individual factors. Using a state-space realization of Ψ , an augmented system H is formed as in (4).

The road profile obeys the bounds $|z_R(t)| \leq \bar{z}_R = 0.3$ m and $|\dot{z}_R(t)| \leq 0.15$ m/s for all $t \geq 0$, which result in $|dz_R(k)| \leq \bar{dz}_R = 0.15T$ for all $k \in \mathbb{N}_0$. Thus, for all $k \in \mathbb{N}_0$, $d(k)$ belongs to the symmetric polytope Γ defined by the vertices $v_1 = (\bar{z}_R, 0)$, $v_2 = (\bar{z}_R - \bar{dz}_R, \bar{dz}_R)$, $v_3 = (-\bar{z}_R, \bar{dz}_R)$, $v_4 = -v_1$, $v_5 = -v_2$, and $v_6 = -v_3$. So, when applying the results of Section 4, we take $d \in \mathbf{D}_\Gamma$, where \mathbf{D}_Γ is defined in (5), and when applying the results of Section 5, we take $d \in \mathbf{D}_\Lambda$, where \mathbf{D}_Λ is defined in (6) and \mathcal{E}_Λ is the minimum volume ellipsoid covering Γ and centered at the origin. Figure 2 shows the schematic diagram and equivalent LFT representation of the uncertain system analyzed in this example.

Theorems 1 and 2 are applied to compute $P \in \mathbb{S}_{++}^{n_G+n_w}$, $W \in \mathbb{S}_{++}^{n_G}$, and $Q \in \mathbb{S}_{++}^{n_y}$ such that if $x_G(0) \in \mathcal{E}_{P_1}$, then $x_G(k) \in \mathcal{E}_W$, $x_H(k) \in \mathcal{E}_P$, and $y(k) \in \mathcal{E}_Q$ for all $k \in \mathbb{N}_0$, $\Delta \in \mathbf{\Delta}$, and $d \in \mathbf{D}_\Gamma$. As explained in Section 4, the matrices P and Q are found in two steps whereby the volume of \mathcal{E}_W is minimized in the first step and that of \mathcal{E}_Q in the second. In the first step, a grid of τ_1 values between $\tau_{1,\min} = 0.99$ and 1 at 10^{-4} increments is used. For $\tau_1 < \tau_{1,\min}$, MOSEK does not return feasible solutions. This $\tau_{1,\min}$ value is found using the bisection method. For our small-scale example, the chosen dense grid of τ_1 values is acceptable. For larger examples, one can perform more efficient gridding by first using coarse grids and then finer grids around the optimal point. In addition to considering the full uncertainty set $\mathbf{\Delta}$, we showcase the modularity of the IQC framework by also considering each uncertainty set alone. That is, we perform the analysis on the three uncertain systems $(G, \mathbf{\Delta}_{\text{SLTI}})$, $(G, \mathbf{\Delta}_{\text{SBN}})$, and $(G, \mathbf{\Delta})$, where G is appropriately defined in each case. Moreover, we apply specialized versions of the results on the nominal discrete-time LTI system G^{nom} without considering any uncertainty, which we obtain by setting $k_{s1} = \bar{k}_{s1}$ and $\bar{u}(k) = K\bar{q}(k)$. In this case, the result for computing the state bounding ellipsoid reduces to that in the Reference 25. The $\tau_{1,\min}$ value changes for the nominal system to 0.985. A summary of the obtained results is presented in Table 1. In the case of the nominal system G^{nom} , there is no need for the formulation of an augmented system nor the IQC machinery, that is, $x_H^{\text{nom}} = x_G^{\text{nom}}$, $P^{\text{nom}} = P_{11}^{\text{nom}} = W^{\text{nom}}$, and $\mathcal{E}_{P^{\text{nom}}}$ defines a state invariant ellipsoid for G^{nom} . Similarly, in the case of $(G, \mathbf{\Delta}_{\text{SBN}})$ wherein the filter Ψ_{SBN} is static, $x_H^{\text{SBN}} = x_G^{\text{SBN}}$, $P^{\text{SBN}} = P_{11}^{\text{SBN}} = W^{\text{SBN}}$, and $x_G(0) \in \mathcal{E}_{P^{\text{SBN}}}$ implies that $x_G(k) \in \mathcal{E}_{P^{\text{SBN}}}$ for all $k \in \mathbb{N}_0$, $\phi \in \mathbf{\Delta}_{\text{SBN}}$, and $d \in \mathbf{D}_\Gamma$. In the case of the uncertain systems $(G, \mathbf{\Delta}_{\text{SLTI}})$ and

TABLE 1 Results from applying Theorems 1 and 2 to the nominal system G^{nom} and the uncertain systems (G, Δ_{SLTI}) , (G, Δ_{SBN}) , and (G, Δ) .

Uncertainty set	$-\log(\det(P))$	$-\log(\det(W))$	$-\log(\det(Q))$
No uncertainty (nominal system)	8.84	8.84	38.42
Δ_{SLTI}	51.13	9.94	38.84
Δ_{SBN}	9.88	9.88	38.72
Δ	54.74	10.93	39.12

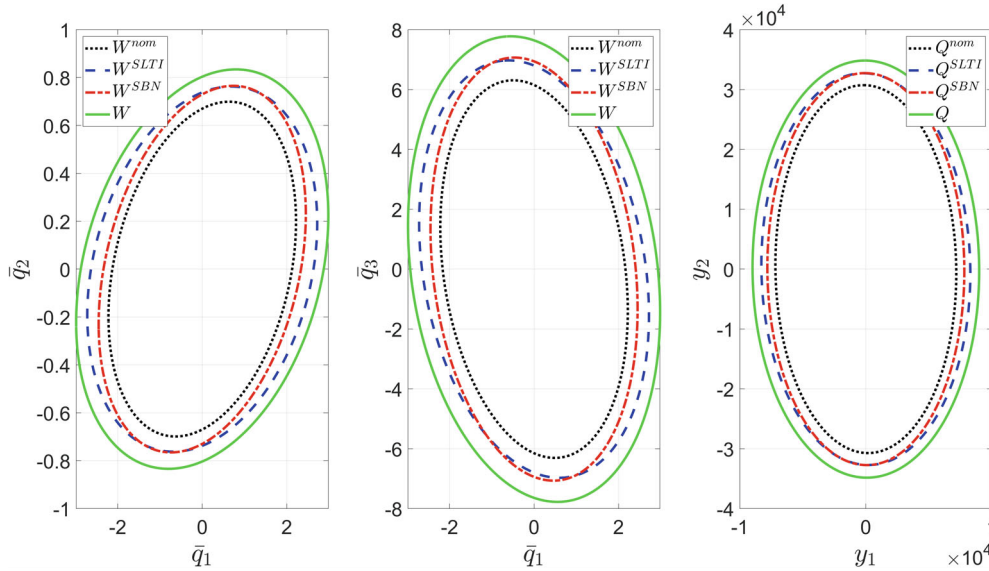


FIGURE 3 Plots of the ellipsoids $\mathcal{E}_{Q^{nom}}$, $\mathcal{E}_{Q^{SLTI}}$, $\mathcal{E}_{Q^{SBN}}$, and \mathcal{E}_Q (right) and the projections of the ellipsoids $\mathcal{E}_{W^{nom}}$, $\mathcal{E}_{W^{SLTI}}$, $\mathcal{E}_{W^{SBN}}$, and \mathcal{E}_W on planes formed by the coordinate axes (left and middle).

(G, Δ) , the filters Ψ_{SLTI} and Ψ are dynamic with $n_\Psi = 6$, and so $n_G + n_\Psi = 10$. In these cases, the volume of \mathcal{E}_W , where $W = P_{11} - P_{12}P_{22}^{-1}P_{12}^T$, is minimized and not that of \mathcal{E}_P . Moreover, the entries in the second column in Table 1 can also be computed from $-\log(\det(P)) = -\log(\det(W)) - \log(\det(P_{22}))$. As expected, the ellipsoids corresponding to the nominal system lie inside those corresponding to the three uncertain systems. As for the ellipsoids corresponding to the three uncertain systems, they compare to each other as follows: $\mathcal{E}_{P^{SLTI}} \subseteq \mathcal{E}_P$, $\mathcal{E}_{W^{SLTI}} \subseteq \mathcal{E}_W$, $\mathcal{E}_{Q^{SLTI}} \subseteq \mathcal{E}_Q$, $\mathcal{E}_{W^{SBN}} \subseteq \mathcal{E}_W$, and $\mathcal{E}_{Q^{SBN}} \subseteq \mathcal{E}_Q$. The output bounding ellipsoids and the projections of the state bounding ellipsoids on the planes (\bar{q}_1, \bar{q}_2) and (\bar{q}_1, \bar{q}_3) are plotted in Figure 3. From the figure, it can be also seen that the ellipsoids $\mathcal{E}_{Q^{SLTI}}$ and $\mathcal{E}_{Q^{SBN}}$ (respectively, $\mathcal{E}_{W^{SLTI}}$ and $\mathcal{E}_{W^{SBN}}$) are not comparable. The scale of the y_1 - and y_2 -axes on the right of Figure 3 is due to the fact that outputs of interest relate to the spring forces in the suspension system.

Next, we illustrate via simulations that the computed ellipsoids for (G, Δ) define bounding sets for x_G , x_H , and y . The simulations are performed on the discrete-time uncertain system. The initial condition $x_G(0)$ for each simulation is computed using a heuristic to start the simulations near the boundaries of both $\mathcal{E}_{P_{11}}$ and \mathcal{E}_Q . Namely, a vector is randomly generated on the boundary of $\mathcal{E}_{P_{11}}$, which is then used to initialize the Matlab solver “fmincon” applied for solving the following nonconvex optimization problem:

$$x_G(0) = \operatorname{argmax}_x \quad x^T C_{G2}^T Q C_{G2} x$$

$$\text{subject to} \quad x^T P_{11} x \leq 1.$$

For each simulation, the uncertain parameter δ_1 is randomly generated in $[-1, 1]$ and the input $d(k)$ is fixed at one of the vertices v_i of Γ for all $k \in \mathbb{N}_0$. As for the nonlinearity ϕ , we consider one of three cases in each simulation: $\phi_1(x) = \alpha x$,

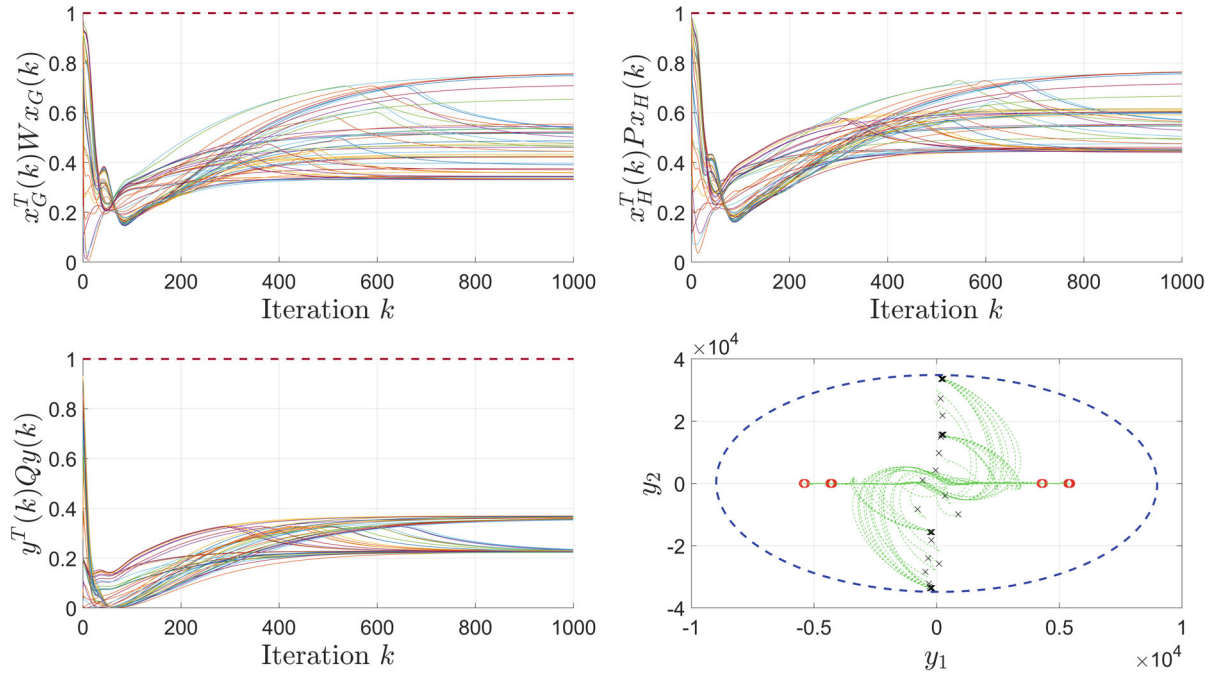


FIGURE 4 Simulation results corresponding to \mathcal{E}_W , \mathcal{E}_P , \mathcal{E}_Q computed by applying Theorems 1 and 2 to system (G, Δ) . In the bottom-right figure, the black “x” and red “o” represent the start and end points of a given simulation, respectively.

TABLE 2 Summary of the results obtained for system (G, Δ) .

Input set	$-\log(\det(P))$	$-\log(\det(W))$	$-\log(\det(Q))$
\mathbf{D}_Γ	54.74	10.93	39.12
Input set	$-\log(\det(\tilde{P}))$	$-\log(\det(\tilde{W}))$	$-\log(\det(\tilde{Q}))$
\mathbf{D}_Λ	59.87	13.69	40.50

Note: Theorems 1 and 2 are applied when $d \in \mathbf{D}_\Gamma$, and Theorem 3 and Corollary 1 are applied when $d \in \mathbf{D}_\Lambda$.

$\phi_2(x) = \beta x$, and

$$\phi_3(x) = \begin{cases} \alpha x, & x \in I_2 \cup I_4, \\ \beta x, & x \in I_1 \cup I_3 \cup I_5, \end{cases}$$

where $I_1 = [-1500, 1500]$, $I_2 = [-3000, -1500] \cup (1500, 3000]$, $I_3 = [-4500, -3000] \cup (3000, 4500]$, $I_4 = [-6000, -4500] \cup (4500, 6000]$, and $I_5 = (-\infty, -6000) \cup (6000, \infty)$. The simulations are shown in Figure 4, where it is seen that $x_G(k) \in \mathcal{E}_W$, $x_H(k) \in \mathcal{E}_P$, and $y(k) \in \mathcal{E}_Q$ for all $k \in \mathbb{N}_0$, as expected, since $x_G(0) \in \mathcal{E}_{P_{11}}$.

Then, Theorem 3 and Corollary 1 are applied to system (G, Δ) to compute $\tilde{P} \in \mathbb{S}_{+++}^{n_G+n_\psi}$, $\tilde{W} \in \mathbb{S}_{+++}^{n_G}$, and $\tilde{Q} \in \mathbb{S}_{+++}^{n_y}$ such that if $x_G(0) \in \mathcal{E}_{\tilde{P}_{11}}$, then $x_G(k) \in \mathcal{E}_{\tilde{W}}$, $x_H(k) \in \mathcal{E}_{\tilde{P}}$, and $y(k) \in \mathcal{E}_{\tilde{Q}}$ for all $k \in \mathbb{N}_0$, $\Delta \in \Delta$, and $d \in \mathbf{D}_\Lambda$. The matrices \tilde{P} and \tilde{Q} are solved for sequentially, and the same grid of τ_1 values is used for $\tilde{\tau}_1$. The results obtained are summarized and compared to those obtained from Theorems 1 and 2 in Table 2. We find that $\mathcal{E}_P \subseteq \mathcal{E}_{\tilde{P}}$, $\mathcal{E}_W \subseteq \mathcal{E}_{\tilde{W}}$, and $\mathcal{E}_Q \subseteq \mathcal{E}_{\tilde{Q}}$, that is, the bounding ellipsoids corresponding to \mathbf{D}_Γ are subsets of those corresponding to \mathbf{D}_Λ . In terms of computational cost, when $d \in \mathbf{D}_\Gamma$, it takes on average 0.1981 s to solve one instance (for a fixed τ_1) of the SDP for finding the state bounding ellipsoid and 0.1156 s to solve the SDP for finding the output bounding ellipsoid. These numbers are 0.2356 and 0.1304 s, respectively, when $d \in \mathbf{D}_\Lambda$. The reported numbers are obtained using the same platform as in Remark 7.

Figures 5 and 6 show the ellipsoids \mathcal{E}_Q and $\mathcal{E}_{\tilde{Q}}$ and the projections of \mathcal{E}_W and $\mathcal{E}_{\tilde{W}}$ on the (\bar{q}_1, \bar{q}_2) and (\bar{q}_1, \bar{q}_3) planes. They also show simulations obtained similarly to those reported in Figure 4. In both figures, the simulations in black

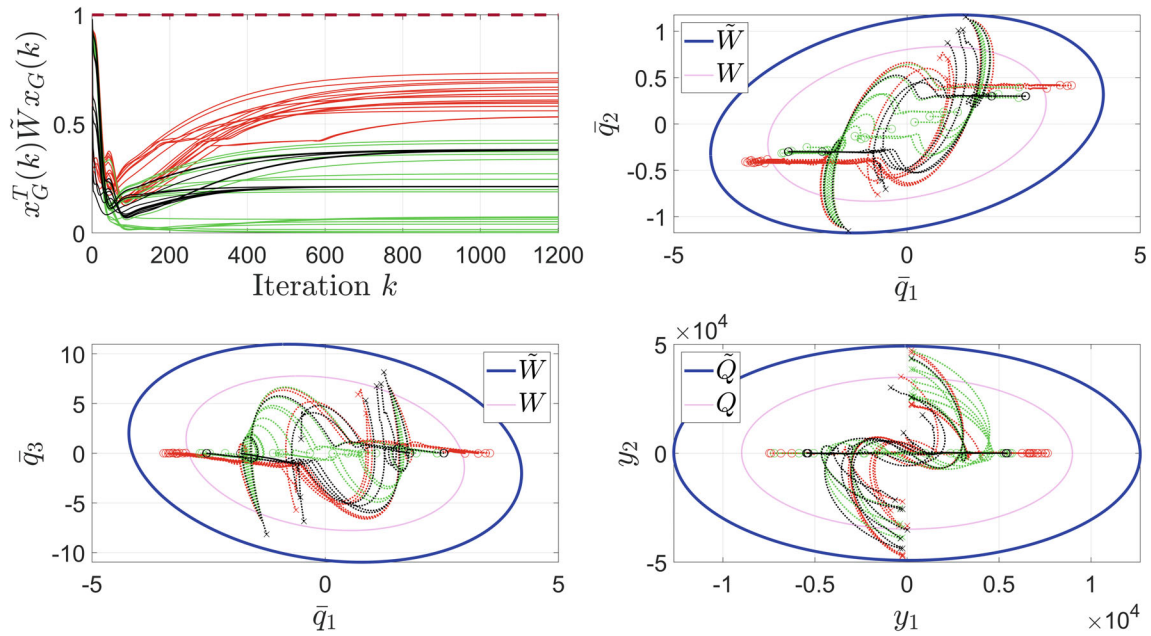


FIGURE 5 Plots of the output bounding ellipsoids \mathcal{E}_Q and $\mathcal{E}_{\tilde{Q}}$ (bottom right) and projections of the state bounding ellipsoids \mathcal{E}_W and $\mathcal{E}_{\tilde{W}}$ on the (\bar{q}_1, \bar{q}_2) and (\bar{q}_1, \bar{q}_3) planes (top right and bottom left, respectively). The figure shows simulations that start from $x_G(0) \in \mathcal{E}_{p_{11}}$ with $d \in \mathbf{D}_\Gamma$ (black) and $d \in \mathbf{D}_\Lambda$ (green and red). The starting and end points of a simulation are marked with “x” and “o,” respectively.

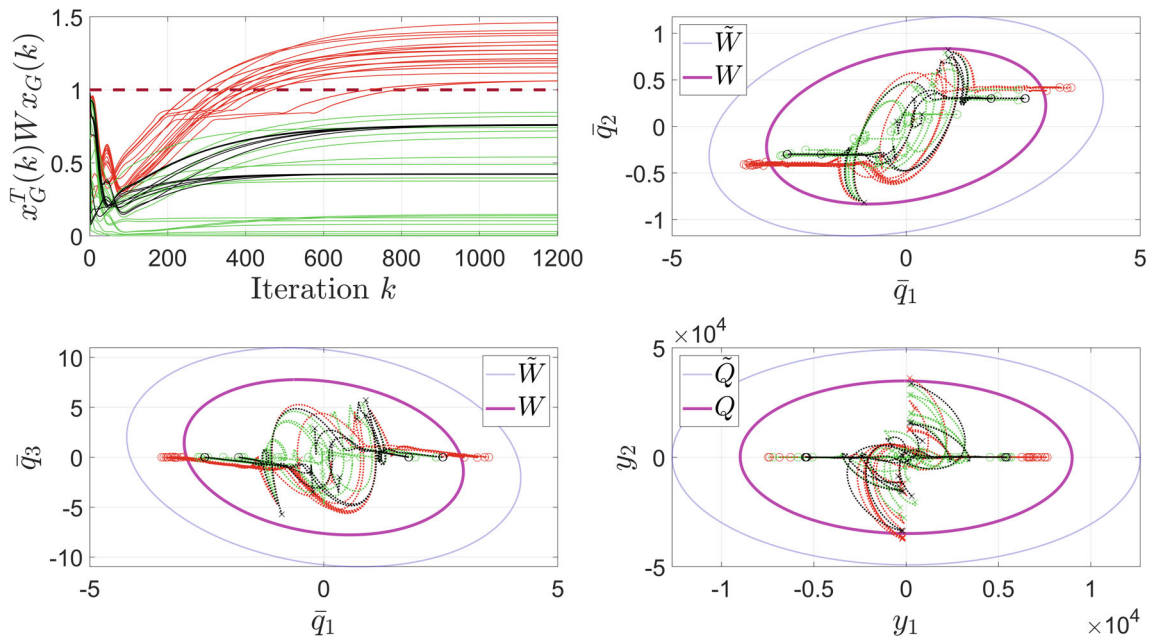


FIGURE 6 Plots of the output bounding ellipsoids \mathcal{E}_Q and $\mathcal{E}_{\tilde{Q}}$ (bottom right) and projections of the state bounding ellipsoids \mathcal{E}_W and $\mathcal{E}_{\tilde{W}}$ on the (\bar{q}_1, \bar{q}_2) and (\bar{q}_1, \bar{q}_3) planes (top right and bottom left, respectively). The figure shows simulations that start from $x_G(0) \in \mathcal{E}_{p_{11}}$ with $d \in \mathbf{D}_\Gamma$ (black) and $d \in \mathbf{D}_\Lambda$ (green and red). The starting and end points of a simulation are marked with “x” and “o,” respectively.

correspond to inputs $d \in \mathbf{D}_\Gamma \subseteq \mathbf{D}_\Lambda$ such that $d(k)$ is fixed at some vertex $v_i \in V$ for all k , while the simulations in red and green correspond to inputs in \mathbf{D}_Λ such that $d(k)$ is fixed at some point on the boundary of \mathcal{E}_Λ for all k . In Figure 5, the simulations start from $x_G(0) \in \mathcal{E}_{P_{11}}$, while the corresponding simulations in Figure 6 (same uncertainties and exogenous input) start from $x_G(0) \in \mathcal{E}_{P_{11}}$. The simulations in Figure 5 show no violations of the bounding ellipsoids, that is, with $x_G(0) \in \mathcal{E}_{P_{11}}$, it can be seen that $x_G(k) \in \mathcal{E}_{\bar{W}}$ and $y(k) \in \mathcal{E}_{\bar{Q}}$ for all k , which is expected since these simulations satisfy the conditions of Theorem 3 and Corollary 1. In Figure 6, the simulations in black show no violations of the bounding ellipsoids, which is also expected since the conditions of Theorems 1 and 2 are satisfied in these simulations. However, violations are observed in the red simulations, wherein $x_G(k)$ and $y(k)$ exit the ellipsoids \mathcal{E}_W and \mathcal{E}_Q , respectively. The green simulations do not happen to exhibit violations of \mathcal{E}_W and \mathcal{E}_Q , but this cannot be guaranteed from our results since $d \in \mathbf{D}_\Lambda \setminus \mathbf{D}_\Gamma$ (set difference of \mathbf{D}_Λ and \mathbf{D}_Γ) in this case, which violates the requirement that $d \in \mathbf{D}_\Gamma$ in Theorems 1 and 2. In other words, when we consider inputs $d(k)$ outside the set Γ , in this case $d(k) \in \mathcal{E}_\Lambda \setminus \Gamma$, we start observing violations of the bounding sets \mathcal{E}_W and \mathcal{E}_Q .

8 | CONCLUSION

This article presents novel methods for computing state and output bounding sets for discrete-time uncertain systems. The exogenous input is assumed to lie in a given polytope or ellipsoid for all time-steps. The uncertainty set is assumed to satisfy a pointwise IQC; and examples of common uncertainty sets that admit such characterizations are given. An example involving the analysis of an active automobile suspension system is given to demonstrate the applicability of the proposed results. Future plans include extending the results to deal with more general quadratic characterizations of uncertainty sets, which renders the results applicable to analysis problems involving neural network controllers. Future work will also tackle the incorporation of pointwise signal IQC characterizations of the input in the results. Other directions for future work may include the study of control invariant sets (and corresponding control laws) for uncertain LFT systems modeled using the IQC framework as well as the consideration of other set representations such as polytopes.

FUNDING INFORMATION

This work is supported by the University Research Board (URB) at the American University of Beirut (AUB), the Office of Naval Research (ONR) under Award No. N00014-18-1-2627, the Army Research Office (ARO) under Contract No. W911NF-21-1-0250, the Center for Unmanned Aircraft Systems under National Science Foundation (NSF) Grant No. CNS-1650465, and ANR project FEANICES ANR-17-CE25-0018.

CONFLICT OF INTEREST STATEMENT

The authors declare no potential conflict of interest.

DATA AVAILABILITY STATEMENT

Data sharing is not applicable to this article as no datasets were generated or analyzed during the current study.

ORCID

Dany Abou Jaoude  <https://orcid.org/0000-0001-8046-0899>

Mazen Farhood  <https://orcid.org/0000-0001-9855-7250>

REFERENCES

1. Megretski A, Rantzer A. System analysis via integral quadratic constraints. *IEEE Trans Automat Contr*. 1997;42(6):819-830.
2. Schwenkel L, Köhler J, Müller MA, Allgöwer F. Dynamic uncertainties in model predictive control: guaranteed stability for constrained linear systems. *2020 59th IEEE Conference on Decision and Control*. IEEE; 2020:1235-1241.
3. Schwenkel L, Köhler J, Müller MA, Allgöwer F. Model predictive control for linear uncertain systems using integral quadratic constraints. *IEEE Trans Automat Contr*. 2023;68(1):355-368.
4. Abou Jaoude D, Farhood M. Guaranteed output bounds using performance integral quadratic constraints. *2020 American Control Conference (ACC)*. IEEE; 2020:1557-1562.
5. Fry JM, Abou Jaoude D, Farhood M. Robustness analysis of uncertain time-varying systems using integral quadratic constraints with time-varying multipliers. *Int J Robust Nonlinear Control*. 2021;31(3):733-758.

6. Fry JM, Farhood M, Seiler P. IQC-based robustness analysis of discrete-time linear time-varying systems. *Int J Robust Nonlinear Control*. 2017;27(16):3135-3157.
7. Scherer CW, Veenman J. Stability analysis by dynamic dissipation inequalities: on merging frequency-domain techniques with time-domain conditions. *Syst Control Lett*. 2018;121:7-15.
8. Fetzner M, Scherer CW, Veenman J. Invariance with dynamic multipliers. *IEEE Trans Automat Contr*. 2018;63(7):1929-1942.
9. Seiler P, Moore RM, Meissen C, Arcak M, Packard A. Finite horizon robustness analysis of LTV systems using integral quadratic constraints. *Automatica*. 2019;100:135-143.
10. Blanchini F, Miani S. *Set-Theoretic Methods in Control*. Systems & Control: Foundations & Applications. 2nd ed. Birkhauser; 2015.
11. Boyd S, Vandenberghe L. *Convex Optimization*. Cambridge University Press; 2004.
12. Chernousko FL. What is ellipsoidal modelling and how to use it for control and state estimation? In: Elishakoff I, ed. *Whys and Hows in Uncertainty Modelling*. Springer; 1999:127-188.
13. Ellipsoidal Toolbox homepage. <https://systemanalysisdpt-cmc-msu.github.io/ellipsoids/>
14. Kurzhanskiy AA, Varaiya P. Computation of reach sets for dynamical systems. In: Levine WS, ed. *The Control Systems Handbook*. 2nd ed. CRC Press; 2011.
15. Li Y, Lin Z. The maximal contractively invariant ellipsoids for discrete-time linear systems under saturated linear feedback. *Automatica*. 2017;76:336-344.
16. García P, Ampountolas K. Robust disturbance rejection by the attractive ellipsoid method—Part II: discrete-time systems. *IFAC-PapersOnLine*. 2018;51(32):93-98.
17. Lam J, Zhang B, Chen Y, Xu S. Reachable set estimation for discrete-time linear systems with time delays. *Int J Robust Nonlinear Control*. 2015;25(2):269-281.
18. Tahir F, Jaimoukha IM. Low-complexity polytopic invariant sets for linear systems subject to norm-bounded uncertainty. *IEEE Trans Automat Contr*. 2015;60(5):1416-1421.
19. Gupta A, Köroğlu H, Falcone P. Computation of low-complexity control-invariant sets for systems with uncertain parameter dependence. *Automatica*. 2019;101:330-337.
20. Gupta A, Köroğlu H, Falcone P. Computation of robust control invariant sets with predefined complexity for uncertain systems. *Int J Robust Nonlinear Control*. 2021;31(5):1674-1688.
21. Althoff M. An introduction to CORA 2015. In: Frehse G, Althoff M, eds. *1st and 2nd International Workshop on Applied Verification for Continuous and Hybrid Systems*. Vol 34. EPiC; 2015:120-151.
22. Althoff M, Frehse G, Girard A. Set propagation techniques for reachability analysis. *Annu Rev Control Robot Auton Syst*. 2021;4(1):369-395.
23. Kochdumper N, Althoff M. Sparse polynomial zonotopes: a novel set representation for reachability analysis. *IEEE Trans Automat Contr*. 2021;66(9):4043-4058.
24. Jönsson UT. A lecture on the S-procedure; 2001.
25. Roux P, Jobredeaux R, Garoche PL, Feron E. A generic ellipsoid abstract domain for linear time invariant systems. *Proceedings of the 15th ACM International Conference on Hybrid Systems: Computation and Control*. ACM; 2012:105-114.
26. Lessard L, Recht B, Packard A. Analysis and design of optimization algorithms via integral quadratic constraints. *SIAM J Optim*. 2016;26(1):57-95.
27. Abou Jaoude D, Garoche PL, Farhood M. Computing state invariants using point-wise integral quadratic constraints and the S-procedure. *2021 American Control Conference (ACC)*. IEEE; 2021:2394-2399.
28. Grymin DJ, Neas CB, Farhood M. A hierarchical approach for primitive-based motion planning and control of autonomous vehicles. *Rob Auton Syst*. 2014;62:214-228.
29. Arifianto O, Farhood M. Optimal control of a small fixed-wing UAV about concatenated trajectories. *Control Eng Pract*. 2015;40:113-132.
30. Feron E. From control systems to control software. *IEEE Control Syst Mag*. 2010;30(6):50-71.
31. Hu B, Lacerda MJ, Seiler P. Robustness analysis of uncertain discrete-time systems with dissipation inequalities and integral quadratic constraints. *Int J Robust Nonlinear Control*. 2017;27(11):1940-1962.
32. Apkarian P, Tuan HD. Parameterized LMIs in control theory. *SIAM J Control Optim*. 2000;38(4):1241-1264.
33. Yin H, Seiler P, Arcak M. Stability analysis using quadratic constraints for systems with neural network controllers. *IEEE Trans Automat Contr*. 2022;67(4):1980-1987.
34. Hindi H, Boyd S. Analysis of linear systems with saturation using convex optimization. *Proceedings of the 37th IEEE Conference on Decision and Control*. IEEE; 1998:903-908.
35. Löfberg J. YALMIP: a toolbox for modeling and optimization in MATLAB. *2004 IEEE International Conference on Robotics and Automation*. IEEE; 2004:284-289.
36. MOSEK ApS. The MOSEK optimization toolbox for MATLAB manual. Version 8.1.0.54; 2018.
37. Muniraj D, Palfaman MC, Guthrie KT, Farhood M. Path-following control of small fixed-wing unmanned aircraft systems with \mathcal{H}_∞ type performance. *Control Eng Pract*. 2017;67:76-91.
38. Veenman J, Scherer CW, Köroğlu H. Robust stability and performance analysis based on integral quadratic constraints. *Eur J Control*. 2016;31:1-32.
39. Köroğlu H, Scherer CW. Robust stability analysis against perturbations of smoothly time-varying parameters. *Proceedings of the 45th IEEE Conference on Decision and Control*. IEEE; 2006:2895-2900.

40. Köroğlu H, Scherer CW. Robust performance analysis for structured linear time-varying perturbations with bounded rates-of-variation. *IEEE Trans Automat Contr.* 2007;52(2):197-211.
41. Belanger PR. *Control Engineering: A Modern Approach*. Saunders College Publishing; 1995.
42. de Oliveira M, Bernussou J, Geromel J. A new discrete-time robust stability condition. *Syst Control Lett.* 1999;37(4):261-265.

How to cite this article: Khalife E, Abou Jaoude D, Farhood M, Garoche P-L. Computation of invariant sets for discrete-time uncertain systems. *Int J Robust Nonlinear Control.* 2023;33(14):8452-8474. doi: 10.1002/rnc.6834